สารเรืองแสงที่ละลายน้ำได้จากไตรฟีนิลเบนซีน

นาย สกรรจ์ ศิริลักษณะพงศ์

วิทยานิพนธ์นี้เป็นส่วนหนึ่งของการศึกษาตามหลักสูตรปริญญาวิทยาศาสตรมหาบัณฑิต
สาขาวิชาปิโตรเคมีและวิทยาศาสตร์พอลิเมอร์
คณะวิทยาศาสตร์ จุฬาลงกรณ์มหาวิทยาลัย
ปีการศึกษา 2553

WATER-SOLUBLE FLUOROPHORES FROM TRIPHENYLBENZENE

Mr. Sakan Sirilaksanapong

A Thesis Submitted in Partial Fulfillment of the Requirements
for the Degree of Master of Science Program in Petrochemistry and Polymer Science
Faculty of Science
Chulalongkorn University
Academic Year 2010

Thesis Title	WATER-SOLUBLE FLUOROPHORES FROM TRIPHENYLBENZENE
By	Mr. Sakan Sirilaksanapong
Field of Study	Petrochemistry and Polymer Science
Thesis Advisor	Assistant Professor Paitoon Rashatasakhon, Ph.D.

Accepted by the Faculty of Science, Chulalongkorn University in Partial Fulfillment of the Requirements for the Master's Degree

…… Dean of the Faculty of Science
(Professor Supot Hannongbua, Dr.rer.nat)

THESIS COMMITTEE

……Chairman
(Associate Professor Supawan Tantayanon, Ph.D.)

……Thesis Advisor
(Assistant Professor Paitoon Rashatasakhon, Ph.D.)

……Examiner
(Associate Professor Voravee Hoven, Ph.D.)

……External Examiner
(Panya Sunintaboon, Ph.D.)

สกรรจ์ ศิริลักษณะพงศ์ : สารเรืองแสงที่ละลายน้ำได้จากไตรเฟนิลเบนซีน
(WATER-SOLUBLE FLUOROPHORES FROM TRIPHENYLBENZENE)
อ. ที่ปรึกษาวิทยานิพนธ์หลัก : ผศ.ดร. ไพฑูรย์ รัชตะสาคร, 54 หน้า.

งานวิจัยนี้เกี่ยวข้องกับการออกแบบและสังเคราะห์สารประกอบเรืองแสงชนิดใหม่จำนวน 3 ตัว โดยสารทุกตัวประกอบด้วยแกนกลางที่เป็น1,3,5-ไตรเฟนิลเบนซีนและมีหน่วยซ้ำเป็นเฟนิลีนเอไทนิลีน แต่มีหมู่รอบนอกที่แตกต่างกัน โครงสร้างถูกประกอบขึ้นโดยอาศัยการทำปฏิกิริยาโซโนกาชิราระหว่างแกนกลางกับหมู่รอบนอกที่มีหมู่ฟังก์ชันเอสเทอร์ อันได้แก่ เอทิล 4-เอไทนิลเบนโซเอท, ไดเอทิล 5-เอไทนิล-ไอโซพทาเลท และ เอทิล 5-ไอโอโดซาลิไซเลท และเมื่อทำปฏิกิริยาไฮโดรไลซิสแล้วจะได้สารประกอบเรืองแสง (**1**-**3**) ที่ละลายน้ำได้ดี การศึกษาสมบัติทางแสงของสารทั้งสามชนิดในสารละลายบัฟเฟอร์ pH 8 ความเข้มข้น 10 มิลลิโมลาร์พบว่าสารทั้งสามสามารถดูดกลืนแสงได้สูงสุดที่ความยาวคลื่นระหว่าง 310 ถึง 318 นาโนเมตร และคายพลังงานแสงสูงสุดที่ความยาวคลื่นในช่วง 375 ถึง 465 นาโนเมตร โดยประสิทธิภาพในการคายพลังงานแสงของสาร**1**, **2** และ **3** เท่ากับ 21.4, 47.2, และ 0.7% ตามลำดับ นอกจากนี้ยังพบว่าสาร **3** ที่มีหมู่ปลายเป็นหมู่ซาลิไซเลต สามารถถูกระงับสัญญาณฟลูออเรสเซนต์ได้ด้วยไอออนของทองแดงได้อย่างจำเพาะเจาะจง โดยในกรณีที่ไม่มีการใช้สารปรับพื้นผิวจะมีค่าคงที่ของการระงับสัญญาณเท่ากับ 1.62×10^{6} $(\text{โมลาร์})^{-1}$ และเมื่อมีการใส่สารปรับพื้นผิวเช่น ไตรตัน X-100 พบว่าจะได้ค่าคงที่ของการระงับสัญญาณสูงถึง 1.50×10^{7} $(\text{โมลาร์})^{-1}$

สาขาวิชา ปิโตรเคมีและวิทยาศาสตร์พอลิเมอร์ ลายมือชื่อนิสิต.....
ปีการศึกษา 2553 ลายมือชื่อ อ.ที่ปรึกษาวิทยานิพนธ์หลัก.....

#5172483823 : MAJOR PETROCHEMISTRY AND POLYMER SCIENCE
KEYWORDS : FLUOROPHORE / TRIPHENYL BENZENE FLUORESCENCE SENSOR/ CU(II) SENSOR / WATER SOLUBLE

SAKAN SIRILAKSANAPONG : WATER-SOLUBLE FLUOROPHORES FROM TRIPHENYLBENZENE ADVISOR: ASST. PROF. PAITOON RASHATASAKHON, Ph.D., 54 pp.

This research involves the design and synthesis of three new fluorophores. All of these compounds have the same 1,3,5-triphenylbenzene core and phenyleneethynylene repeating units but different peripheral groups. The fluorophore structures were composed by Sonogashira reaction between the core and peripheral parts with ester functional groups such as ethyl 4-ethynylbenzoate, diethyl 3-ethynyl-isophthalate, and ethyl 5-iodosalicylate. Upon hydrolysis, the water-soluble fluorophores **1**-**3** were obtained. The photophysical studies in 10 mM phosphate buffer pH 8 revealed that these compounds have maximum wavelength of absorption between 310 and 318 nm and can emit the light in the wavelength range of 375-465 nm. The emission efficiencies of compound **1**, **2**, and **3** are 21.4, 47.2, and 0.70%, respectively. In addition, it was found that the fluorescent signal of compound **3** with salicylate peripheries could be selectively quenched by Cu^{2+} ion. In the absence of surfactant, the quenching constant is 1.62×10^{6} M^{-1}. This value can be increased up to 1.50×10^{7} M^{-1} by the addition of surfactant such as Triton X-100.

Field of Study : Petrochemistry and Polymer Science Student's Signature .....
Academic Year : 2010 Advisor's Signature .....

ACKNOWLEDGEMENTS

First of all, I would like to express my sincere gratitude to my thesis advisor, Assistant Professor Paitoon Rashatasakhon, Ph.D. for valuable advice, guidance and kindness throughout this research. Sincere thanks are also extended to Associate Professor Supawan Tantayanon, Ph.D., Associate Professor Voravee Hoven, Ph.D. and Panya Sunintaboon, Ph.D., attending as the committee members, for their valuable comments and suggestions.

I would like to especially thank Associate Professor Mongkol Sukwattanasinitt, Ph.D. for valuable guidance and Prof. Thawatchai Tuntulani for kind support on the UV/Vis and fluorescence spectrometers.

In particular, I am thankful to the Center for Petroleum, Petrochemicals, and Advanced Materials, The 90th Anniversary of Chulalongkorn University Fund, National Nanotechnology Center (NN-B-22-FN9-10-52-06) and Faculty of Science, Chulalongkorn University (A1B1-5) for supporting my thesis. Gratitude is also extended to the members of my research group for their helpful discussion.

Finally, I would like to specially thank my family and friends for their encouragement and understanding throughout. I would not be able to reach this success without them.

CONTENTS

CHAPTER **Page**

CHAPTER **Page**

LIST OF TABLES

LIST OF FIGURES

LIST OF SCHEMES

LIST OF ABBREVIATIONS

Ar	aromatic
calcd	calculated
^{13}C NMR	carbon-13 nuclear magnetic resonance
$CDCl_3$	deuterated chloroform
DMSO- d_6	deuterated dimethyl sulfoxide
DMSO	dimethylsulfoxide
d	doublet (NMR)
dd	doublet of doublet (NMR)
ESIMS	electrospray ionization mass spectrometry
equiv	equivalent (s)
FT-IR	fourier transform infrared spectroscopy
g	gram (s)
^{1}H NMR	proton nuclear magnetic resonance
Hz	Hertz
HRMS	high resolution mass spectrum
h	hour (s)
IR	infrared
J	coupling constant
mg	milligram (s)
mL	milliliter (s)
mmol	millimole (s)
m/z	mass per charge
m	multiplet (NMR)
M.W.	molecular weight
M	molar
MHz	megaHerz
rt	room temperature
s	singlet (NMR)
THF	tetrahydrofuran
TLC	thin layer chromatography

UV	ultraviolet
δ	chemical shift
°C	degree Celsius
µL	microliter (s)
µM	micromolar (s)
Φ	quantum yield
% yield	percentage yield

CHAPTER I

INTRODUCTION

1.1 Fluorescence

Fluorescence is the emission of light that typically occurs with aromatic compounds or highly conjugated molecules. The process occurs after the molecules absorb energy in the form of light, which can usually be illustrated by the Jablonski diagram (**Figure 1.1**) [1]. The singlet ground, first, and second electronic states are depicted by S0, S1, and S2, respectively. At each of these electronic energy levels, the fluorophores can exist in a number of vibrational energy levels, depicted by 0, 1, 2, etc. Upon the absorption of light energy, the fluorophore is usually excited to some higher vibrational level of either S1 or S2. With a few rare exceptions, molecules in condensed phases rapidly relax to the lowest vibrational level of S1. This process is called internal conversion and generally occurs within 10^{-12} s or less. Since fluorescence lifetimes are typically near 10^{-8} s, internal conversion is generally completed prior to the emission. Hence, fluorescence emission generally results from a thermally equilibrated excited state, that is, the lowest energy vibrational state of S1.

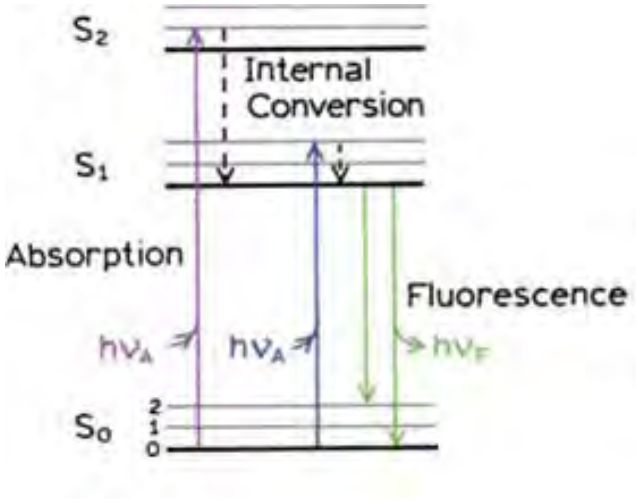

Figure 1.1 Jablonkski diagram

Some typical fluorescent substances (fluorophores) are shown in **Figure 1.2**. The colors from which the fluorophores emit depend on the structures and substituents. These compounds are examples of small-molecule fluorophores. However, conjugated polymeric fluorophores such as poly(phenyleneethynylene), poly(phenylenevinylene) and poly(fluorene) are often found their applications as signal transducers in fluorescent sensors [2].

Small-molecule fluorophores

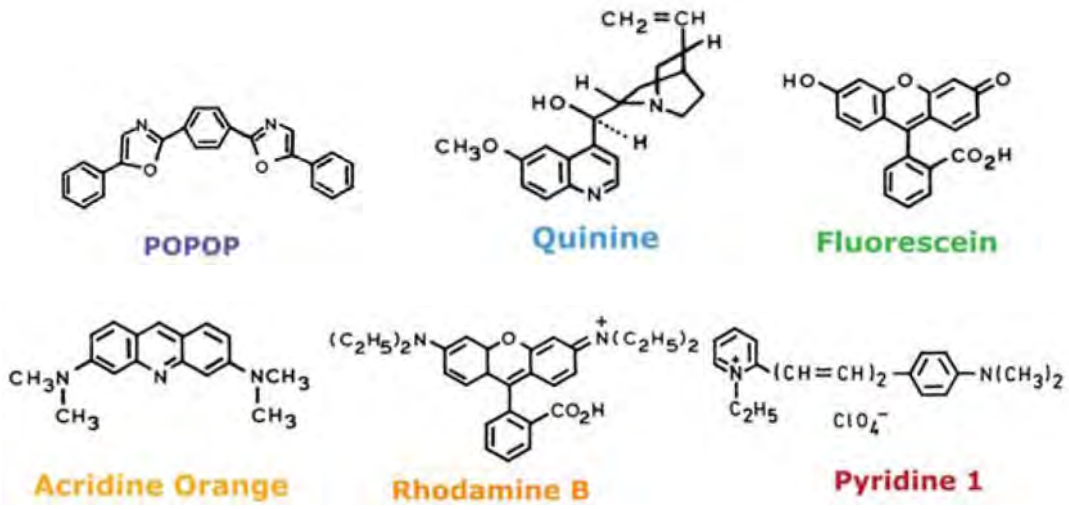

Conjugated polymer

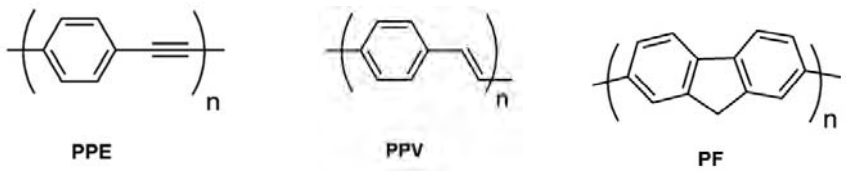

Figure 1.2 Small-molecule and conjugated polymer fluorescent compounds.

1.2 Fluorescent chemosensor

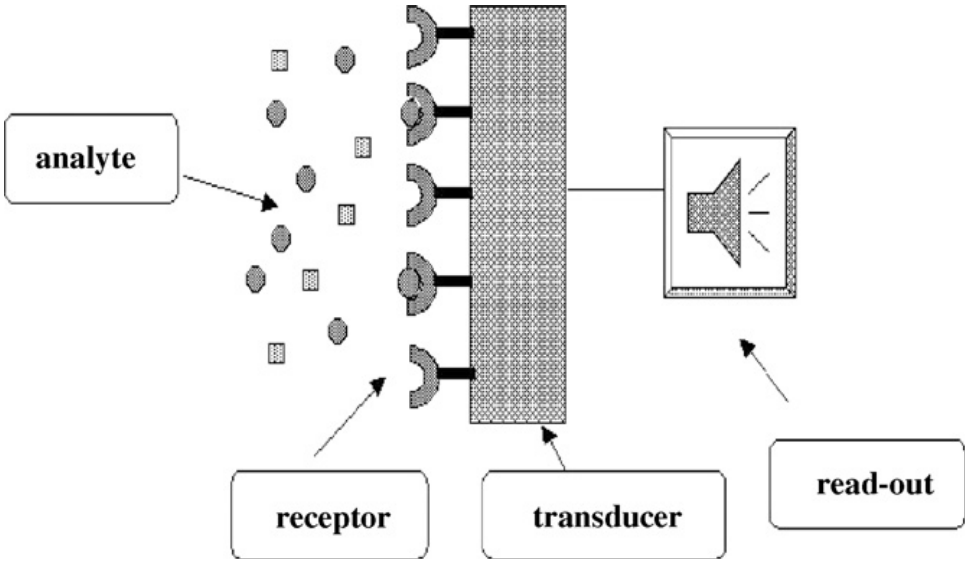

Figure 1.3 The three components of fluorescent chemosensor

In general, sensors are composed of three major components: a receptor, a transducer, and a read-out [3]. For the fluorescent sensors, a fluorophore functions as the signal transducer and a fluorometer is the read-out part that records and monitors the change in fluorescent signals. For the purpose of chemical detection and quantitative analysis, the most important part of chemosensors is a selective molecular recognition that can result in changes of photophysical property. Most of the fluorescent ion sensors are composed of an ion recognition unit (ionophore) for selective binding of the substrate, while the fluorogenic unit (fluorophore) provides the means of signaling this bonding, whether by fluorescence quenching or enhancement. The combination of these two words is also called for “fluoroionophore”. The mechanism which controls the response of a fluoroionophore to substrate binding includes photo-induced electron transfer (PET), photo-induced charge transfer (PCT), fluorescence (Förster) resonance energy transfer (FRET), and excimer/exciplex formation or extinction.

1.3 Fluorescent quenching

Fluorescence quenching refers to any process that decreases the fluorescence intensity of a sample. There are a wide variety of quenching processes that include excited state reactions, molecular rearrangements, ground state complex formation, and energy transfer. Quenching experiments can be used to determine the accessibility of quencher to a fluorophore, monitor conformational changes, or monitor association reactions of the fluorescence of one of the reactants changes upon binding. There are two basic types of quenching: dynamic (collisional) and static quenching. Both types require an interaction between the fluorophore and quencher. In the case of dynamic quenching the quencher must diffuse to the fluorophore during the lifetime of the excited state, and upon contact the fluorophore, returns to the ground state without emission of a photon. In the case of static quenching, a non-fluorescent complex is formed between the fluorophore and the quencher. The formation of this complex does not rely upon population of the exited state.

1.3.1 Stern-Volmer plot

Linear dependence quenching data are usually presented as plots of F_0/F versus $[Q]$; in which F_0 is the initial fluorescent intensity, F is the observed fluorescent intensity after the addition of quencher, and $[Q]$ is the concentration of quencher. This plot should yield an intercept of unity on the y axis and a slope equal to K_{SV} (the Stern-Volmer constant). Examples of this plot are shown in **Figure 1.4**. It is useful to note that $1/K_{SV}$ is the quencher concentration at which $F_0/F = 2$, or 50% of the intensity is quenched. A linear Stern-Volmer plot is generally indicative of a single class of fluorophores that are all equally accessible to the quencher. If two fluorophore populations are present, and one class is not accessible to quencher, then the Stern-Volmer plots deviate from linearity toward the x-axis (downward). This result is frequently found for the quenching of tryptophan fluorescence in proteins by polar or charged quenchers [4].

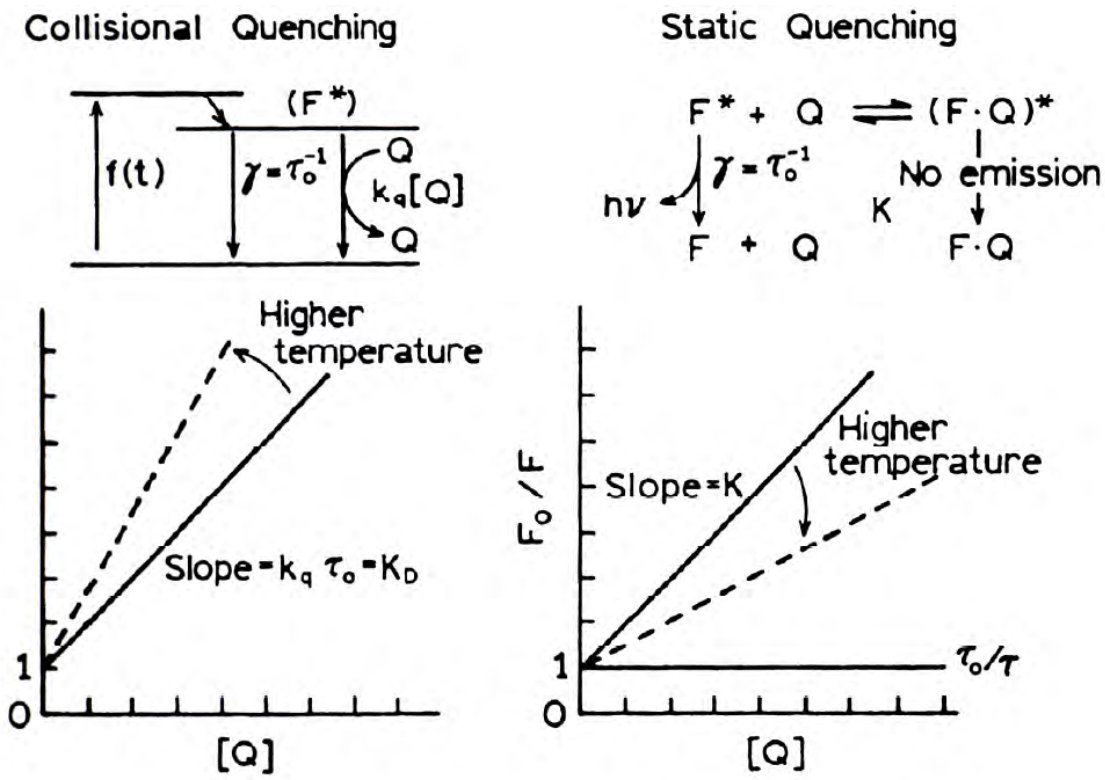

Figure 1.4 Collisional (left) and static quenching (right).

1.3.2 Collisional quenching

Collisional quenching occurs when the excited-state fluorophore is deactivated upon contact with some other molecule in solution, which is called the quencher. In this case the fluorophore is returned to the ground state during a diffusive encounter with the quencher. The molecules are not chemically altered in the process. For collisional quenching, the decrease in intensity is described by the well-known Stern-Volmer equation:

$$\frac{F_0}{F} = 1+K[Q] = 1+ k_q\tau_0[Q] \quad (1)$$

where *Fo* and *F* are the fluorescent intensity in the absence and presence of quencher, *K* is the Stern-Volmer quenching constant, *kq* is the bimolecular quenching constant, τ_0 is the lifetime in the absence of quencher and [*Q*] is the quencher concentration. The Stern-Volmer constant is sometimes abbreviated as $K_{SV.}$

1.3.3 Static quenching

Static quenching involves the formation of a complex between the quencher and fluorophore that does not rely on diffusion in the excited state. The dependence of the fluorescence intensity upon quencher concentration for static quenching is derived by consideration of the association constant for complex formation.

$$K_S = \frac{[FQ]}{[F][Q]} \tag{2}$$

Where K_S is the fluorophore-quencher association constant, $[FQ]$ is the concentration of the complex, $[F]$ is the concentration of the uncomplexed fluorophore, and $[Q]$ is the concentration of quencher. Since the total concentration of the fluorophore, $[F]_T$ is given by $[F]_T = [F] + [FQ]$, the static quenching constant can be written as

$$Ks = \frac{[F]_T[F]}{[F][Q]} - \frac{[F]_T}{[F][Q]} - \frac{1}{[Q]} \tag{3}$$

which can be rearranged to

$$\frac{[F_0]}{[F]} = 1 + Ks[Q] \tag{4}$$

By recognizing the fluorescence signal in the absence of quencher, F_0 would correspond to the total concentration of fluorophore, one can substitute the fluorescence intensities F_0 and F for the total and free concentrations $[F]_T$ and $[F]$, respectively to obtain:

$$\frac{F_0}{F} = 1 + Ks[Q] \tag{5}$$

which is exactly the same linear equation we used for dynamic quenching.

1.4 Literature review on fluorescent chemosensors

Examples of literatures related to fluorescent sensors for metal ions during the last 5 years are as follows:

In 2006, Kim and Bunz [5] studied the use of poly(phenyleneethynylene), PPE(**I**) and several proteins on the detection of metal ion. They found that the combination of PPE(**I**) and papain was a highly sensitive fluorescent sensor for Hg^{2+}. In the absence of papain, the Hg^{2+} ion can quenched the fluorescent signal of PPE(**I**) with a K_{SV} of $1.3x10^{4}$ M^{-1}. Upon on addition of papain, the quenching efficiency increased to $5.6x10^{5}$ M^{-1}. This signal amplification resulted from the Hg^{2+}-induced agglutination of complex between PPE(**I**) and papain.

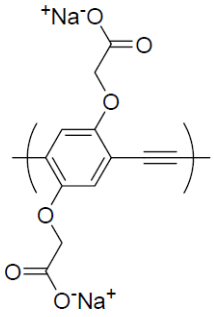

I

Figure 1.5 Carboxylate-Substituted PPE (**I**)

Later in the same year, a group of Chinese researchers [6] reported the use of bipyridine ruthenium complex **II** as a fluorescent sensor for Cu^{2+} by quenching process. The complex responded well toward Cu^{2+} in the concentration range from $5x10^{-8}$ M to $1.0x10^{-4}$ M with a detection limit of $4.2x10^{-8}$ M. The quenching mechanism was proposed as a complexation between Cu^{2+} and the carboxylate group of the sensor.

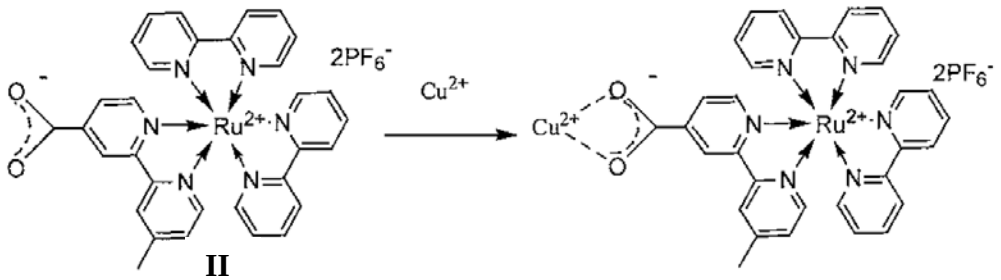

II

Figure 1.6 Bipyridine ruthernium complex (**II**)

In 2007, Weng and coworkers [7] demonstrated the use of porphyrin-zinc complex (**III**) as a selective sensor for Cu^{2+}. The study was conducted in organic solution (The CH_2Cl_2/MeOH (20:1) and detection limit was $1.5x10^{-6}$ M with a K_{sv} = $6.31x10^5$ M^{-1} The selectivity of this sensor could not be interfered by addition of other metal ions.

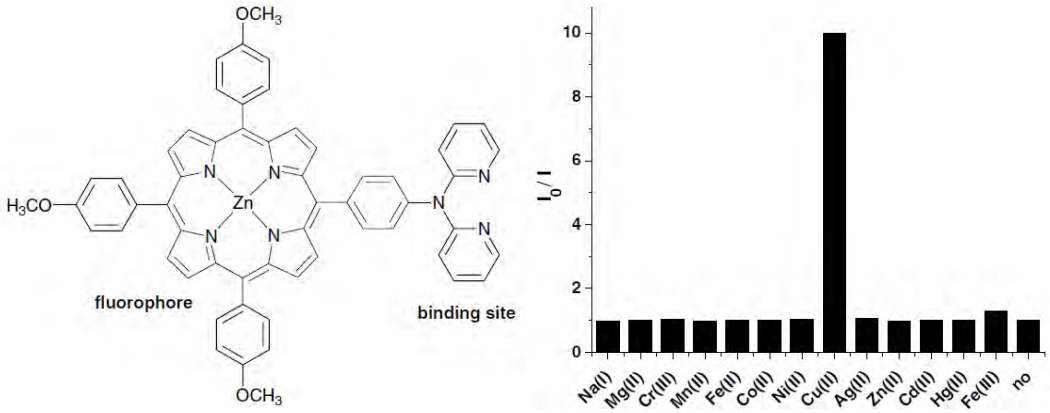

III

Figure 1.7 Structure of **III** and responses toward metal ions

In the same year, Ha-Thi and coworkers [8] reported that the fluorescent molecular sensor for Hg^{2+} based on the phosphane sulfide derivative, 1,2-bis(diphenyl thiophosphinophenyl)ethane (**IV**) exhibited a very low detection limit in an aqueous medium (3.8 nM). The effect of cation complexation was then studied in CH_3CN/ H_2O (80:20) at pH 4, and the **IV** has quantum yield = 0.1. The selectivity of **IV** over other cations such as Ca^{2+}, Na^+, K^+, Mg^{2+}, Pb^{2+}, Cd^{2+}, Cu^{2+}, Ag^+, and Zn^{2+} was evaluated.

No significant change of the fluorescence was observed upon addition of a large excess of these interfering cations.

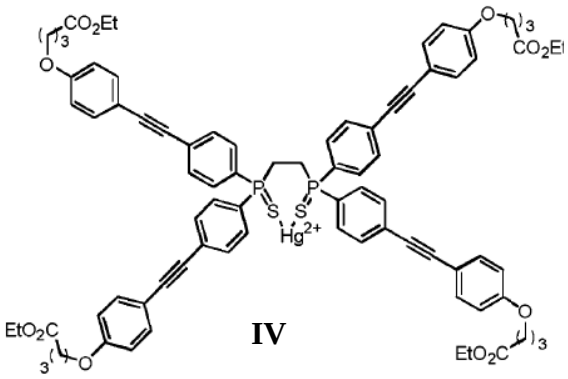

IV

Figure 1.8 Structure of 1,2-bis(diphenyl thiophosphinophenyl)ethane

In 2008, Tolosa and coworkers [9] synthesized water soluble fluorescent cruciforms **V-VII** The emission spectra of these compounds shifted differently upon the addition of metal ions such as Mg^{2+}, Ca^{2+}, Al^{3+}, Hg^{2+}, Zn^{2+}, Fe^{2+} and Cu^{2+}. This responsive property was developed into a sensor array for metal ions.

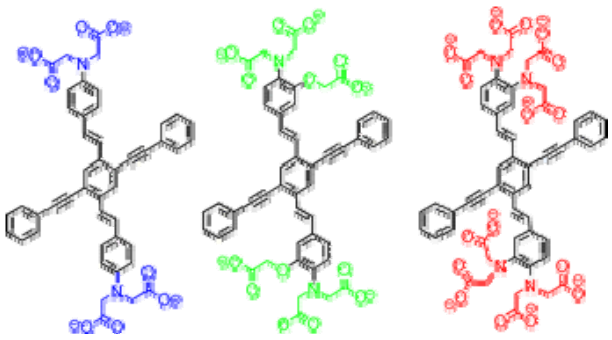

V **VI** **VII**

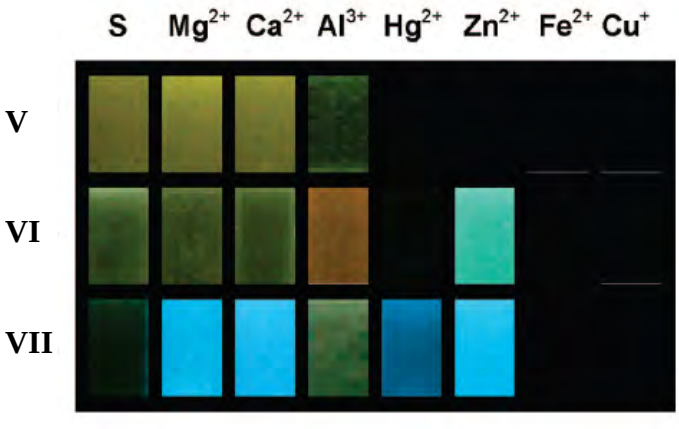

Figure 1.9 Fluorogenic responses of **V**-**VII** in the presence of metal ions.

In 2009, Jung and coworkers [10] synthesized a novel coumarin-based fluorogenic probe bearing the 2-piconyl unit (**VIII**) as a fluorescent chemosensor with selectivity toward Cu^{2+}. The receptor can be applied to monitoring Cu^{2+} ion in aqueous solution (HEPES/DMSO, 9:1) with pH span of 4-10. The fluorescent changes of this compound were studied with Cu^{2+} concentration range of 0-50 μM and the detection limit was estimated to be 0.5 μM.

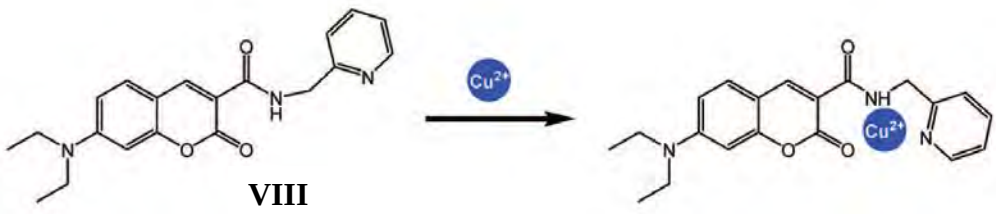

VIII

Figure 1.10 Structure of coumarin derivative (**VIII**) and proposed the mechanism with Cu^{2+}

In 2009, Xu and coworkers [11] developed a Zn^{2+} selective fluorescent sensor naphthalimide based fluorescent probe ZTRS which contains an amide-PDA receptor, **IX** that has strongest affinity with Zn^{2+} among competitive metal ions such as Fe^{2+}, Co^{2+}, Ni^{2+}, Cu^{2+}, Cd^{2+} and Hg^{2+} and displays an excellent fluorescent selectivity for Zn^{2+} - triggered amide tautomerization. **IX** can bind to both Zn^{2+} and Cd^{2+}, these metal ions can be the sensor, green and blue fluorescence were observed, respectively in aqueous solution (CH_3CN/0.5 M HEPES pH 7.4, 50:50).

IX

Figure 1.11 The structure of **IX** and its fluorogenic responses toward Cd^{2+} and Zn^{2+}

In 2009, Niamnont and coworkers [12] reported the synthesis and sensing properties of water soluble fluorescent dendritic compound **X**. This dendritic compound composed of phenylene-ethynylene repeating units and anionic carboxylate peripheries. Without a surfactant, compound **X** exhibited a low fluorescent quantum yield, but a good selectivity toward Hg^{2+}. After adding Triton X-100, the quantum yield was drastically increased and the sensitivity for the detection of Hg^{2+} was also improved.

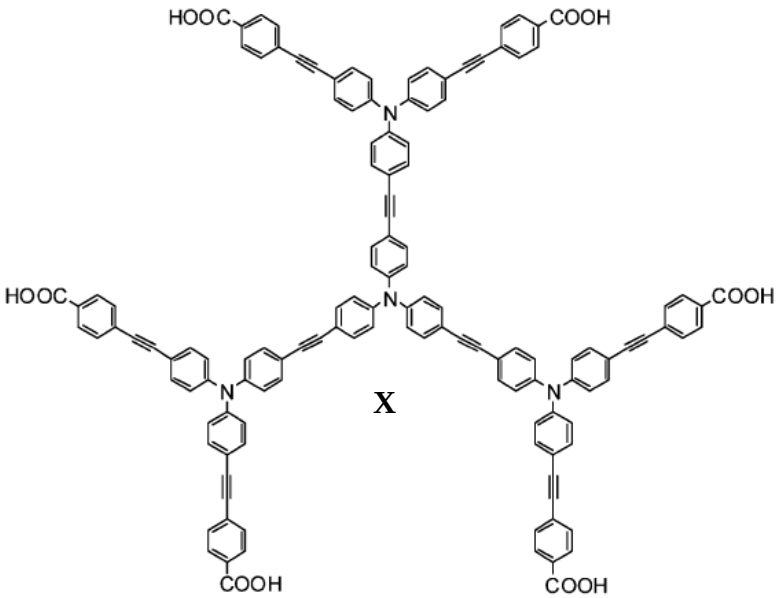

X

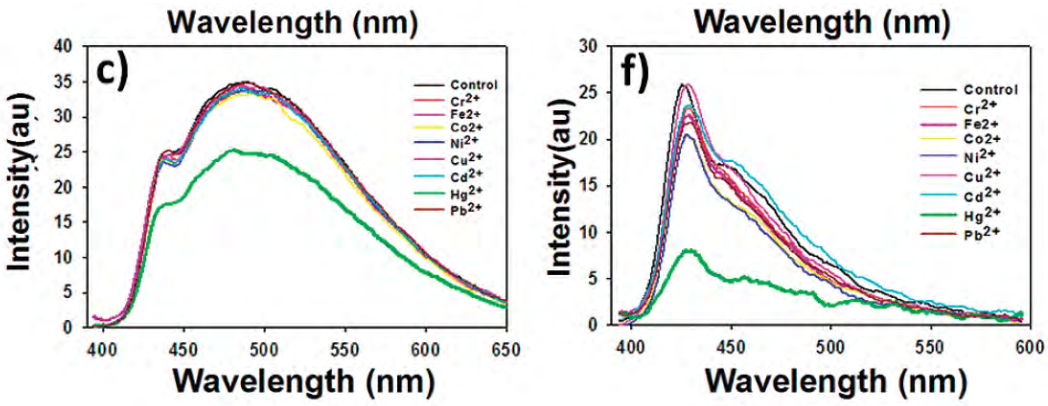

Figure 1.12 Dendritic fluorophore **X** and its selectivity toward Hg^{2+} ion before and after the surfactant added.

1.5 Objectives of this research

The research involved a design and synthesis of three new water soluble fluorophores derived from 1,3,5-triphenylbenzene (**1-3**) (**Figure 1.13**). All compounds contained diphenylacetylene repeating units with different carboxylate peripheries. The photophysical properties as well as the application of these compounds for Cu^{2+} sensor in aqueous media were also investigated.

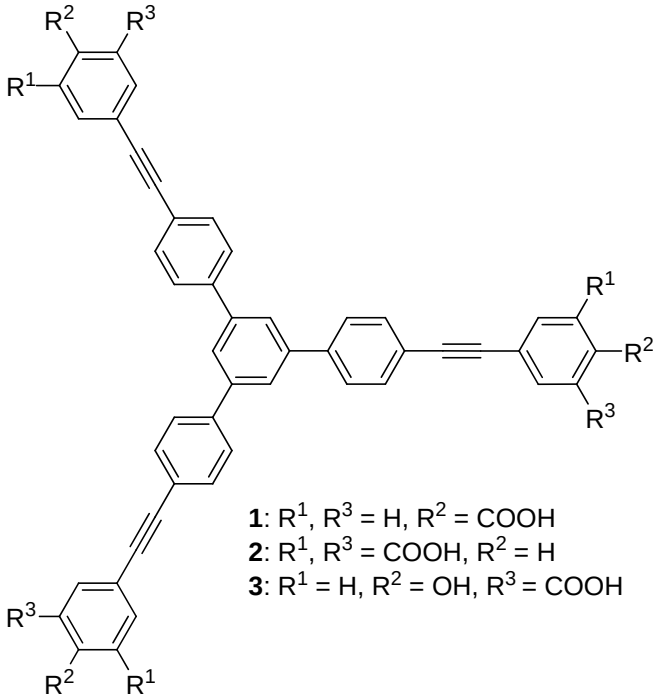

Figure 1.13 Target molecule **1-3**

CHAPTER II

EXPERIMENTAL

2.1 Materials and chemicals

All reagents were purchased from Sigma-Aldrich, Fluka® (Switzerland) or Merck® (Germany). For general reactions, solvents such as methylene chloride (CH_2Cl_2) and acetonitrile (MeCN) were reagent grade stored over molecular sieves. In anhydrous reactions, solvents such as tetrahydrofuran (THF) and toluene (PhMe) were dried and distilled before use according to the standard procedures. All column chromatography were operated using silica gel 60 (70-230 mesh), Merck®. Thin layer chromatography (TLC) was performed on silica gel plates (Merck F_{245}). Solvents such as CH_2Cl_2, hexane, ethyl acetate (EtOAc) and methanol (MeOH) used for extraction and chromatography were commercial grade and distilled before use. Diethyl ether (Et_2O) and chloroform ($CHCl_3$) used for extraction was reagent grade. De-ionized water was used in all fluorescence experiments unless specified otherwise. All reactions were carried out under positive pressure of N_2 filled in rubber balloons.

2.2 Analytical instruments

The compounds were characterized by a melting point apparatus (Electrothermal 9100, Fisher Scientific, USA). Elemental (C, H, N) analysis was performed on PE 2400 series II (Perkin-Elmer, USA). The HRMS spectra were measured on an electrospray ionization mass spectrometer (microTOF, Bruker Daltonics). Fourier transform infrared spectra were acquired on Nicolet 6700 FT-IR spectrometer equipped with a mercury-cadminum telluride (MCT) detector (Nicolet, USA). ^{1}H-NMR spectra were recorded on Varian Mercury 400 MHz NMR spectrometer (Varian, USA) using $CDCl_3$ and DMSO-d_6. ^{13}C-NMR spectra were recorded at 100 MHz on Bruker 400 MHz NMR spectrometer using the same solvent. The UV-Visible spectra were obtained from a Varian Cary 50 UV-Vis

spectrophotometer (Varian, USA) using water, $CDCl_3$ and DMSO-*d*6 as a solvent. Fluorescence emission spectra were acquired by using Perkin Elmer precisely LS 45 Luminescence Spectrometer (PerkinElmer, UK) for metal ion sensor and using a Varian Cary Eclipse spectrofluorometer (Varian, USA) for photophysical property study.

2.3 Synthesis procedures

1,3,5-Tris-(4-iodophenyl)-benzene **(4)**

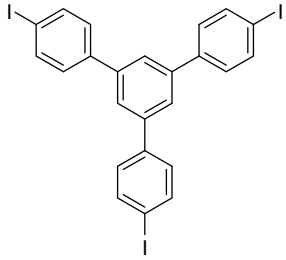

A solution of 4-iodoacetophenone (1.0 g, 4.08 mmol) and CF_3SO_3H (90 µL, 1.00 mmol) in PhMe was stirred under reflux conditions for 3 h. The volatile solvents were removed by evaporation and the residue was purified by column chromatography on silica gel using hexane/CH_2Cl_2 (4:1) as the eluent. The product was further purified by crystallization in EtOH/CH_2Cl_2 (1:1) to afford **4** as white needles (0.65 g, 60 %). ^{1}H NMR (400 MHz, $CDCl_3$): δ 7.78 (d, J = 8.1 Hz, 6H), 7.67 (s, 3H), 7.39 (d, J = 8.1 Hz, 6H). This spectral data agreed with the results reported in the literature [13].

1,3,5-Tris-(4-trimethylsilylethynyl-phenyl)-benzene **(5)**

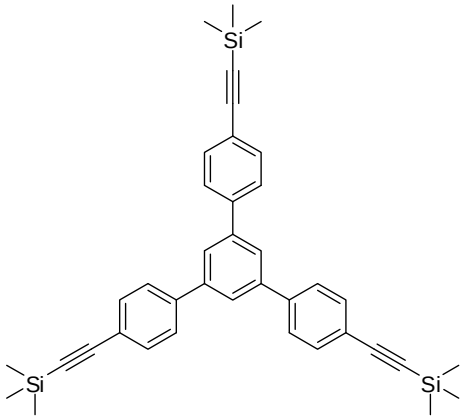

To a de-gassed solution of **4** (1 g, 1.46 mmol) in THF (50 mL) and Et_3N (50 mL) were added $Pd(PPh_3)_2Cl_2$ (154 mg, 220 μmol), PPh_3 (116 mg, 440 μmol) and CuI (84 mg, 440 μmol). Trimethylsilylacetylene (0.7 mL, 4.8 mmol) was slowly added and the reaction mixture was stirred for 5 hours at room temperature. Then the solution was partitioned between CH_2Cl_2 (300 mL) and 6 M HCl (200 mL). The organic phase was separated, washed with saturated NH_4Cl and dried over Na_2SO_4. After evaporation of CH_2Cl_2, the crude product was purified by column chromatography using hexane/CH_2Cl_2 (5:1) as the eluent to afford **5** (850 mg, 97%) as colorless crystals. ^{1}H NMR (400 MHz, $CDCl_3$): δ = 7.80 (s, 3H), 7.67 (d, J = 8.4 Hz, 6H), 7.56 (d, J = 8.4 Hz, 6H), 0.27 (s, 27H); This spectral data agreed with the results reported in the literature [14].

1,3,5-Tris-(4-ethynyl-phenyl)-benzene) **(6)**

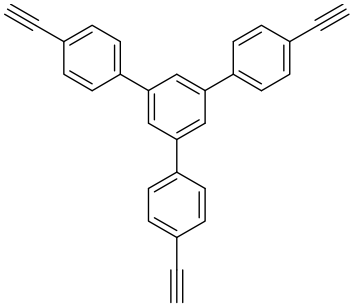

Compound **5** (1.0 g, 1.7 mmol) was dissolved in THF (20 mL) and MeOH (80 mL), then K_2CO_3 (1.4 g, 10.13 mmol) was added. The reaction mixture was stirred for 3 hours. CH_2Cl_2 (300 mL) was added and the organic phase was washed with water, separated, dried over Na_2SO_4, filtered, and concentrated. The crude product was purified by column chromatography (hexane/CH_2Cl_2; 10:3) to afford **6** (460 mg, 85%) as colorless solid. ^{1}H-NMR (400 MHz, $CDCl_3$): δ = 7.81 (s, 3H), 7.70 (d, J = 8.4 Hz, 6H), 7.62 (d, J = 8.4 Hz, 6H), 3.23 (s, 3H). This spectral data agreed with the results reported in the literature [14].

***Triester* (7)**

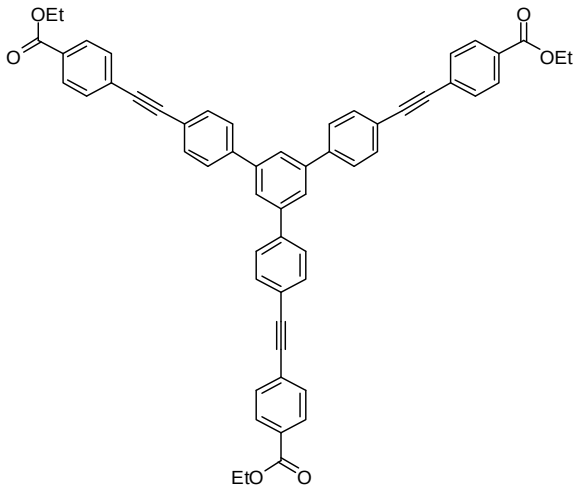

To a de-gassed solution of **4** (100 mg, 0.14 mmol) in THF (10 mL) and Et_3N (10 mL) were added $Pd(PPh_3)_2Cl_2$ (15 mg, 22 μmol), PPh_3 (12 mg, 44 μmol) and CuI (8.4 mg, 44 μmol). A solution of ethyl 4-ethynylbenzoate [15] (100 mg, 0.58 mmol) in THF (2 mL) was added dropwise then stirred overnight. After removal of solvents under reduced pressure, the residue was extracted with H_2O/CH_2Cl_2. The organic phase was washed with brine and dried over Na_2SO_4. The CH_2Cl_2 was removed under reduced pressure and the residue was purified by column chromatography on silica gel using hexane/CH_2Cl_2 (1:4) as the eluent. The tri-ester **7** (93 mg, 78%) was obtained as a pale yellow solid. ^{1}H NMR (400 MHz, $CDCl_3$): δ 8.05 (d, J = 8.4 Hz, 6H), 7.82 (s, 3H), 7.69 (dd, J = 8.17 and 20.26 Hz, 12H), 7.62 (d, J = 8.4 Hz, 6H), 4.39 (q, J = 7.1 Hz, 6H), 1.41 (t, J = 7.1 Hz, 9H); ^{13}C NMR (100 MHz, $CDCl_3$): δ = 166.1, 141.7, 141.0, 132.3, 131.5, 129.9, 129.5, 127.8, 127.3, 125.3, 122.2, 92.1, 89.7, 61.2, 14.3.

Compound 1

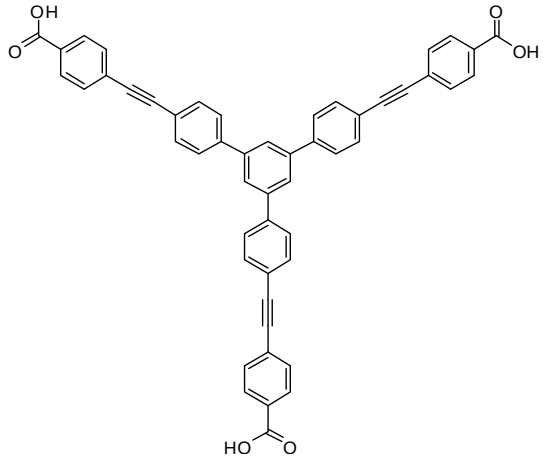

To a solution of **7** (93 mg, 0.69 mmol) in THF (4 mL) and EtOH (4 mL) was added saturated KOH aqueous solution (0.1 mL) and the mixture was refluxed for 6 h. The volatile solvents were evaporated and the residue dissolved in water (5 mL). The solution was cooled with ice and acidified to pH 3 by 1 M HCl. The suspension was centrifused to afford **1** as a yellow solid (79 mg, 90%). ^{1}H NMR (400 MHz, DMSO-d_6): δ 8.04 (s, 3H), 8.00 (dd, J = 8.4 and 17.5 Hz, 12H), 7.71 (t, J = 8.4 Hz, 12H). ^{13}C NMR (100 MHz, DMSO-d_6): δ 166.7, 140.7, 140.3, 132.1, 131.8, 131.5, 130.6, 129.6, 127.6, 126.6, 124.8, 121.2, 115.2, 91.9, 89.5.

Hexaester (8)

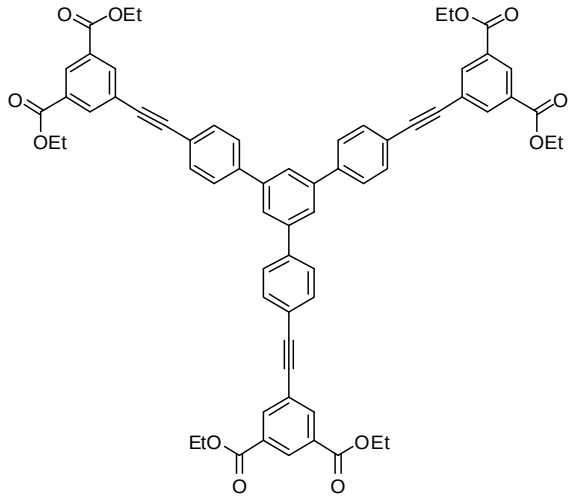

This compound was prepared from **4** (100 mg, 0.14 mmol) and diethyl 5-ethynylisophthalate [16] (120 mg, 0.51 mmol) using the same procedure described for **7**. After purification by a column chromatography using hexane/CH_2Cl_2 (1:2) as the eluent, hexa-ester (**8**) (110 mg, 87%) was obtained as a pale yellow solid. ^{1}H NMR (400 MHz, $CDCl_3$): δ = 8.66 (t, *J* =1.8 Hz, 3H) 8.41 (t, *J* = 1.8 Hz, 6H), 7,86 (s, 3H), 7.77 (t, *J* = 1.8 Hz, *J* = 6.6 Hz, 6H), 7.70 (dd, *J* = 1.8 and 6.6 Hz, 6H), 4.46 (q, *J* = 7.2 Hz, 12H), 1.46 (t, *J* = 7.2 Hz, 18H); ^{13}C NMR (100 MHz, $CDCl_3$): δ 165.2, 141.7, 141.1, 136.4 ,132.3, 131.3, 130.1, 127.4, 125.3, 124.2, 122.0, 90.9, 88.5, 61.6, 14.3.

Compound 2

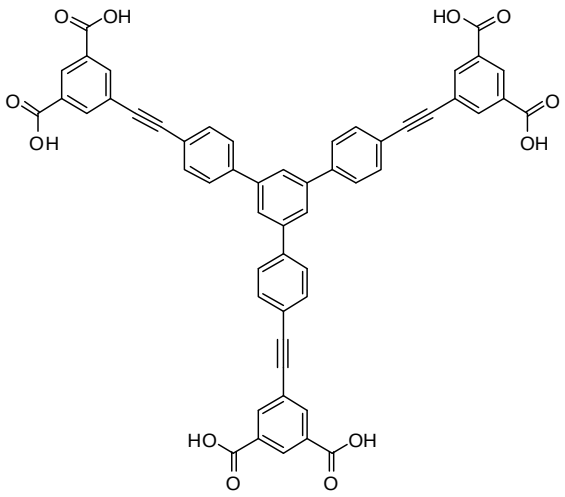

This compound was prepared by hydrolysis of **8** (110 mg) under the method described above as synthesize compound **1**. After the suspension was centrifused, **2** was obtained as a brown solid (95 mg, 96%). ^{1}H NMR (400 MHz, DMSO-d_6): δ 8.46 (t, *J* = 1.5 Hz, 3H), 8.29 (d, *J* = 1.5 Hz, 6H), 8.07 (s, 3H), 8.04 (d, *J* = 8.4 Hz, 6H), 7.77 (d, *J* = 8.4 Hz, 6H). ^{13}C NMR (100 MHz, DMSO-d_6): δ 166.0, 140.7, 140.3, 135.3, 132.7, 132.2, 129.2, 127.6, 124.8, 123.1, 121.1, 90.7, 88.5.

***Tri-salicylate ester* (9)**

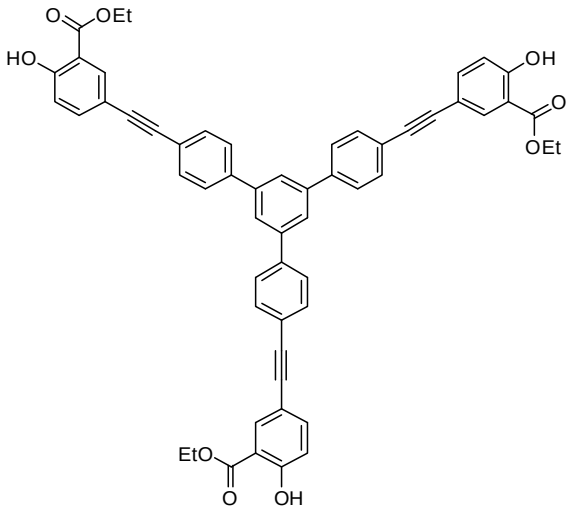

A mixture of ethyl 5-iodosalicylate [18] (0.25 g, 0.872 mmol) and THF/*i*Pr_2NH (3mL/1 mL) was de-gassed with N_2 gas. $Pd(PPh_3)_2Cl_2$ (5.5 mg, 2 mol%) and CuI (3 mg, 6 mol%) were added and the mixture stirred at 25 °C for 10 min. A solution of **6** (0.1 g, 0.26 mmol) in anhydrous THF (1 mL) was then added dropwise and mixture stirred 3.5 h at 50 °C. Upon completion, volatile materials were removed under reduced pressure, and the residue added to water (10 mL), which was extracted with CH_2Cl_2. The organic phase was washed with water and then brine, and dried over $NaSO_4$. The CH_2Cl_2 was removed under reduced pressure and the resulting solid purified by column chromatography on silica gel using CH_2Cl_2/hexane (1:1) to afford the salicylate ester **9** (0.154 g, 68%) as a pale grey solid. ^{1}H NMR (400 MHz, $CDCl_3$): δ 11.02 (s, 3H), 8.08 (s, 3H), 7.81 (s, 3H), 7.67 (dd, J = 26.84, 7.66 Hz, 15H), 6.99 (d, J = 7.85 Hz, 3H), 4.45 (q, J = 6.17 Hz, 6H), 1.46 (t, J = 6.92 Hz, 9H) ^{13}C NMR (100 MHz, DMSO-d_6): δ 161.7, 141.7, 140.5, 138.5, 133.4, 132.0, 127.3, 127.2, 125.1, 122.7, 118.0, 115.0, 114.2, 112.8, 89.4, 88.0, 61.8, 14.2

Compound 3

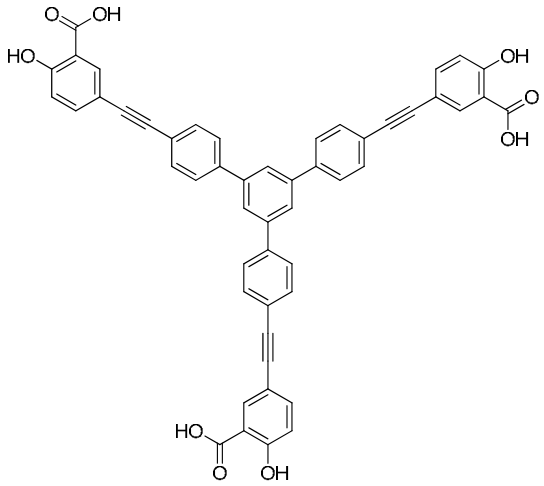

This compound was prepared by hydrolysis of **9** (110 mg) under the method described above as synthesize compound **1**. After the suspension was centrifused, **3** was obtained as a grey solid (100 mg, 98%). 1H NMR (400 MHz, DMSO-d_6) δ 8.00 (dd, J = 13.89, 5.59 Hz, 15H), 7.69 (t, J = 8.49 Hz, 12H), 7.02 (d, J = 8.44 Hz, 3H) ^{13}C NMR (100 MHz, DMSO-d_6): δ 170.9, 161.2, 140.7, 139.7, 137.9, 133.5, 131.7, 127.4, 124.5, 121.8, 117.9, 113.9, 112.9, 89.4, 87.99. Anal. Calcd. for $C_{51}H_{30}O_9$ (786.78): C 77.85, H 3.84; found C 77.58, H 3.82.

2.4 Photophysical property study

The stock solutions of compound (**1**, **2** and **3** (~20 μM)) was prepared by dissolve each compound with phosphate buffer (PB, 10 mM) pH 8.0 in volumetric flask 100 mL.

2.4.1 UV-Visible spectroscopy

The UV-Visible absorption spectra of the stock solutions of **1**, **2** and **3** were recorded from 200 nm to 700 nm at ambient temperature.

2.4.2 Fluorescence spectroscopy

The stock solutions of compounds **1**, **2** and **3** were diluted to 20 μM, phosphate buffer 10 mM pH8. The emission spectra of three compounds were

recorded from 300 nm to 700 nm at ambient temperature using an excitation wavelength at 318, 310 and 316 nm for compound **1**, **2** and **3** respectively.

2.4.3 Fluorescence quantum yields

The fluorescence quantum yield of compounds **1**, **2** and **3** were performed in PB phosphate buffer (PB, 10 mM) pH 8.0 by using 2-aminopyridine in 0.1 M H_2SO_4 (Φ = 0.60) and quinine sulphate in 0.1 M H H_2SO_4 (Φ = 0.54) as a reference. The UV-Visible absorption spectra of five analytical samples and five reference samples at varied concentrations were recorded. The maximum absorbance of all samples should never exceed 0.1. The fluorescence emission spectra of the same solutions using appropriate excitation wavelengths selected were recorded based on the absorption maximum wavelength (λ_{max}) of each compound. Graphs of integrated fluorescence intensities were plotted against the absorbance at the respective excitation wavelengths. Each plot should be a straight line with 0 interception and gradient *m*.

In addition, the fluorescence quantum yield (Φ) was obtained from plotting of integrated fluorescence intensity *vs* absorbance represented into the following equation:

$$\Phi_X = \Phi_{ST}\left(\frac{Grad_X}{Grad_{ST}}\right)\left(\frac{\eta_X^2}{\eta_{ST}^2}\right)$$

The subscripts Φ_{ST} denote the fluorescence quantum yield of a standard as a reference. Φ_X is the fluorescence quantum yield of sample and η is the refractive index of the solvent.

2.5 Fluorescent sensor study

2.5.1 Surfactant enhancement

The stock solution of compound **3** with a concentration of 10 mM in phosphate buffer pH 8.0 was prepared. The emission spectrum of **3** was recorded from 300 nm to 700 nm at ambient temperature using an excitation wavelength at 316

nm and the photophysical properties were studied by use 3 surfactants of non-ionic surfactant. The stock surfactants were prepared in phosphate buffer (PB, 10 mM) pH 8.0. Concentrations of all stock surfactants were adjusted to 30 μM and were added with the desired volumes (0-100 μL) to the fluorophore solutions. The final volumes of the mixtures were adjusted to 5 mL.

2.5.2 Metal ion sensor

The stock solutions of **1**, **2** and **3** with a concentration of 10 mM in phosphate buffer pH 8.0 were prepared. The emission spectrum of **3** was recorded from 300 nm to 700 nm at ambient temperature using an excitation wavelength at 300 nm and the photophysical properties were studied for 19 metal ions with and without non-ionic surfactants. Metal acetate and sulfate solutions were prepared in Milli-Q water. Concentrations of all stock metal acetate and sulfate solutions were adjusted to 100 μM and were added with the desired volumes (0-500 μL) to the fluorophore solutions. The final volumes of the mixtures were adjusted to 5 mL.

CHAPTER III

RESULTS AND DISSCUSTION

3.1 Synthesis and characterization

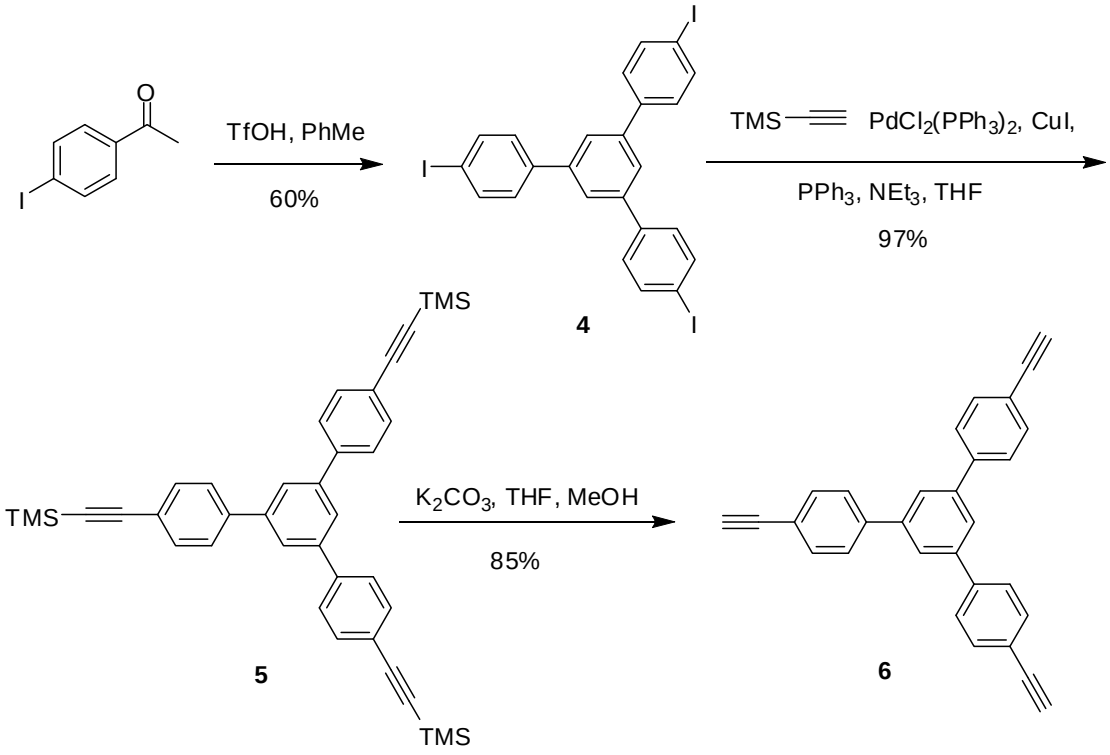

Scheme 3.1 Synthesis of 1,3,5-triphenylbenzene cores

The synthesis of fluorophore **1-3** began with the cyclotrimerization of 4-iodoacetophenone catalyzed by trifluoromethanesulfonic acid that afforded triiodo triphenylbenzene **4** in 60% yield (**Scheme 3.1**). Subsequent Sonogashira coupling with trimethylsilylacetylene provided tri-yne **5** in excellent yield of 97%. The protective silyl groups were removed upon treatment with potassium carbonate in THF and MeOH.

For the construction of fluorophores (**Scheme 3.2**), the peripheral units – ethyl 4-ethynylbenzoate [15], diethyl 5-ethynylisophthalate [16], and ethyl 5-ethynylsalicylate [17] – were prepared according to the literature procedures. The Sonogashira coupling between triiodo core **4** with the peripheral units successfully produced triester **7** and hexaester **8** in 78 and 87% yield, respectively. Unfortunately,

attempt to couple ethyl 5-ethynylsalicylate with **4** gave rise to a complex mixture with a little formation of **9**. To circumvent this problem, the tri-yne core **6** was reacted with ethyl 5-iodosalicylate [18] under the Sonogashira reaction conditions and the expected compound (**9**) was afforded in moderate yield of 68%. Base-catalysed hydrolysis of **7**-**9** resulted in the desired fluorophores **1**-**3** in 90, 96, and 98% yield, respectively.

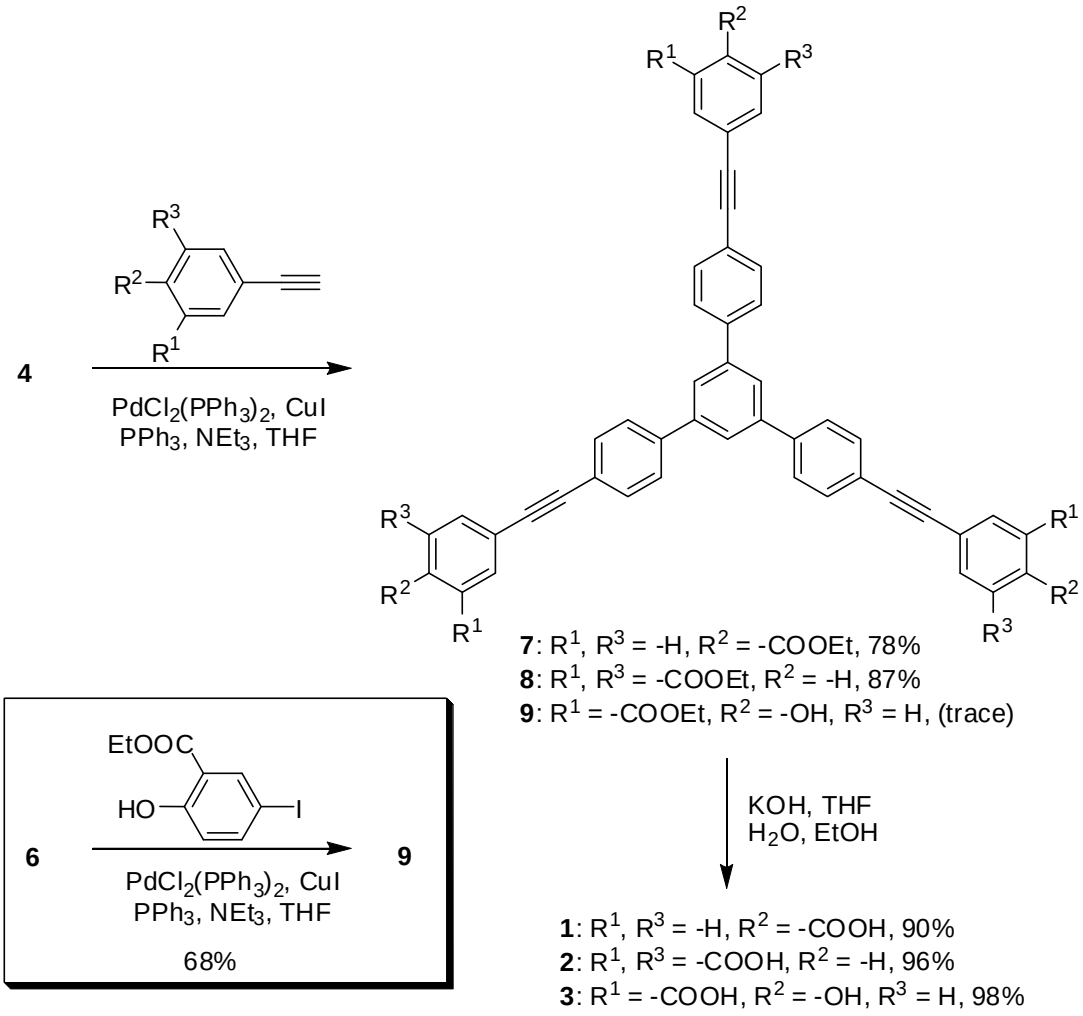

Scheme 3.2 Synthesis of fluorophore **1**-**3**.

3.2 Photophysical property

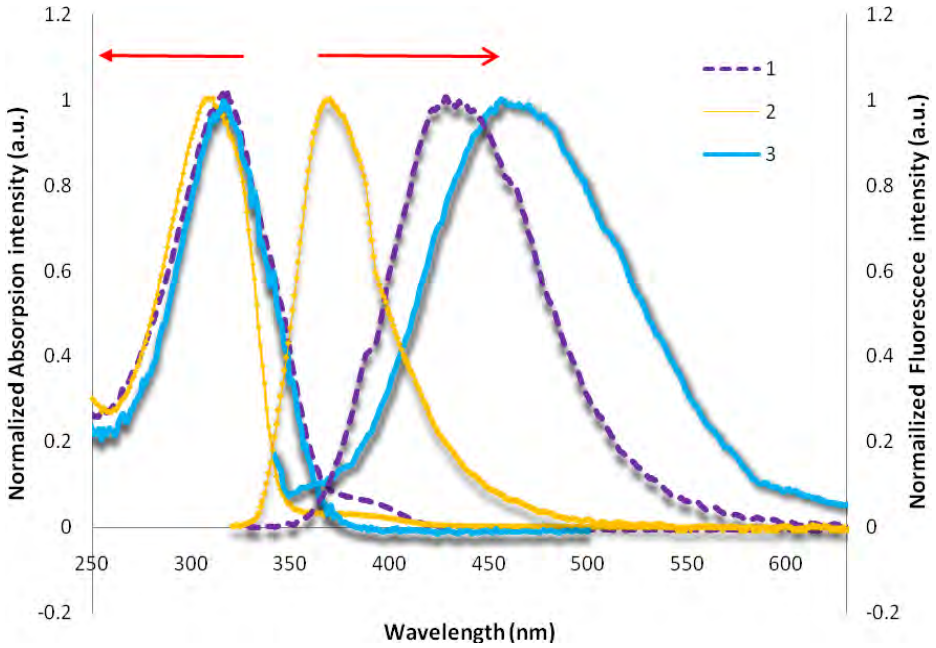

Figure 3.1 Normalized absorption and emission spectra of compound **1**, **2** and **3** in 10 mM phosphate buffer pH 8.

Table 3.1. Photophysical properties of **1-3** in 10 mM phosphate buffer pH 8.0.

Cmpd.	Absorption		Emission	
	λ_{abs} (nm)	ε (M^{-1} cm^{-1})	λ_{ems} (nm)	Φ
1	318	47000	426	0.214 [a]
2	310	19600	365	0.472 [a]
3	316	19000	465	0.007 [b]

[a] 2-Aminopyridine in 0.1 M H_2SO_4 (Φ = 0.60) and [b] Quinine sulphate in 0.1 M H_2SO_4 (Φ = 0.54) were used as references.

The normalized intensity of absorption and fluorescence spectra of compound **1- 3** are presented in **Figure 3.1** and tabulated in **Table 3.1**. The three fluorophores showed maximum wavelength of absorption around 310 – 318 nm. The effect of substitution patterns at the peripheries could be observed as these compounds

exhibited significantly different Stokes shifts. The fact that the absorption spectra and the absorption maxima of the three compounds appeared at almost the same wavelength suggested that these compounds have a similar π-conjugated system. However, it was found that **1** has the highest molar extinction coefficients. It is possible that **1** is the least polar fluorophore and could aggregate upon dissolving in aqueous solution. Even though the sample solution of **1** in phosphate buffer is clear and transparent to the human eyes, there might be some small particles of **1** that absorb or scatter UV light and cause the excessive absorption. In the case of **2** and **3**, they could dissolve well in phosphate buffer and, therefore, the molar extinction coefficients are very similar.

For the emission properties, the maximum emission wavelengths of **1-3** were at 426, 365, and 465 nm, respectively. In comparison with fluorophore **2**, the emission band of **1** appeared at a longer wavelength, which indicated that the three carboxylate groups at the *para* positions may cause an intra-molecular charge transfer (ICT). Therefore, the excited state geometry of **1** could be much different from its ground state. Other hand, the carboxylate groups in **2** were positioned at the *meta* positions where the electron-withdrawing groups played less prominent roles. The emission band of **3** was much broader, which may result from the higher ICT between carboxylate groups at the *meta* position and hydroxyl groups at *para* position in aqueous media. The quantum yields (Φ) were determined by using a comparative method with well-characterized standard samples of known quantum yield values and had the emission range cover in emission of compound. For **1** and **2**, 2-aminopyridine in 0.1 M H_2SO_4 with a quantum yield of 0.60 was used as the standard, whereas quinine sulphate in 0.1 M H_2SO_4 (Φ = 0.54) was the standard for the fluorophore **3** because they had the emission range in the range of standard. From **Table 3.1**, it is shown that the highest quantum yield of 47% was obtained from **2,** while the compound **1** possesses a slightly lower value of 21%. This different quantum efficiency may result from the different in water solubility. Fluorophore **2** which has six ionizable carboxylic acid groups was expected to be more polar and hence dissolves in water much better than **1**. For fluorophore **3**, the peripheral units which contain both electron donor (-OH) and electron acceptor (-COOH) may be the cause

of a drastically low quantum yield. It is possible that the intramolecular charge transfer (ICT) could occur with the excited state of **3**.

3.3 Metal ion sensor

To evaluate the sensing properties of fluorophore **1-3** for metal ions, the fluorescent signal of solutions of each fluorophore in phosphate buffer pH 8.0 were monitored in the presence of sixteen metal ions including Na^{+}, Ca^{2+}, Sr^{2+}, Ba^{2+}, Mn^{2+}, Fe^{2+}, Fe^{2+}, Co^{2+}, Ni^{2+}, Cu^{2+}, Zn^{2+}, Zr^{2+}, Ag^{+}, Cd^{2+}, Hg^{2+} and Pb^{2+}. It was found that the fluorescent signals of **1** and **2** could not be altered by any of these metal ions (**Figure 3.2** and **3.3**). Surprisingly, the signal of **3** could be selectively quenched by the addition of Cu^{2+} ion. (**Figure 3.4** and **3.5**). Even with the additional types of cations such as Li^{2+}, K^{+} and Mg^{2+}, the selectivity was still very exclusive toward Cu^{2+}. The selectivity of this fluorescence quenching is probably due to the effect of chelation of Cu^{2+} by the pheripheral hydroxylate-carboxylate groups.

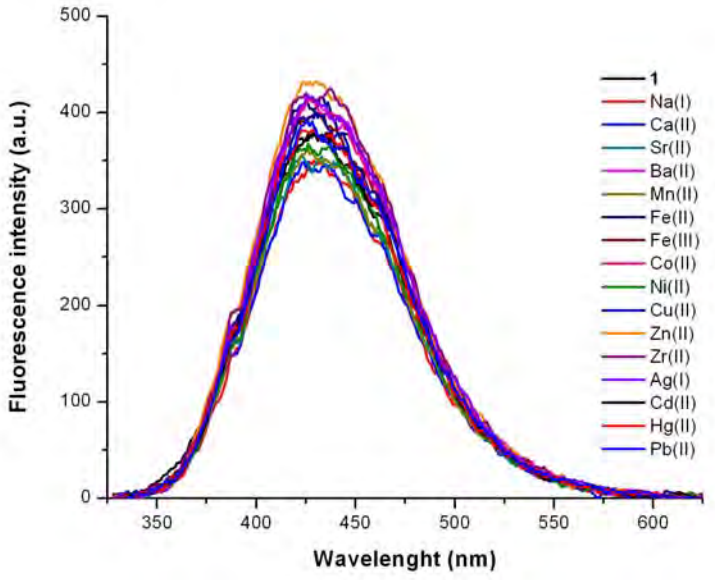

Figure 3.2 Fluorescence spectra of **1** (1 μM) in the presence of 16 metal ions (10 μM).

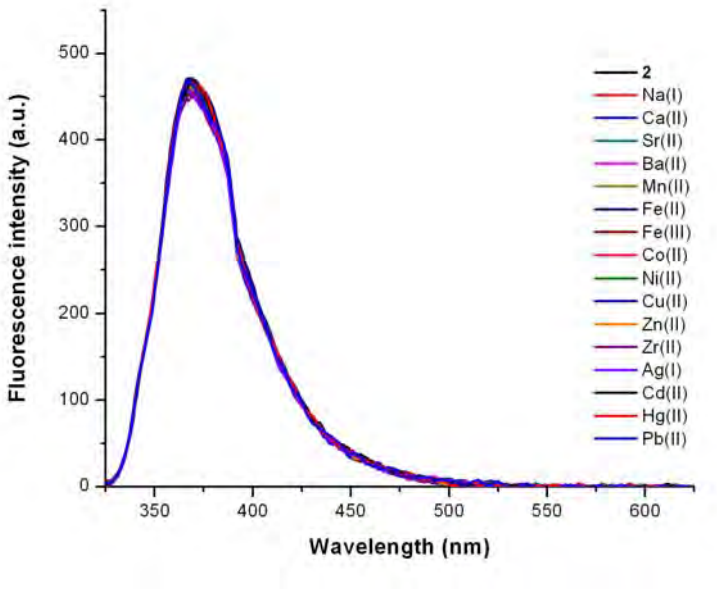

Figure 3.3 Fluorescence spectra of **2** (1 μM) in the presence of 16 metal ions (10 μM).

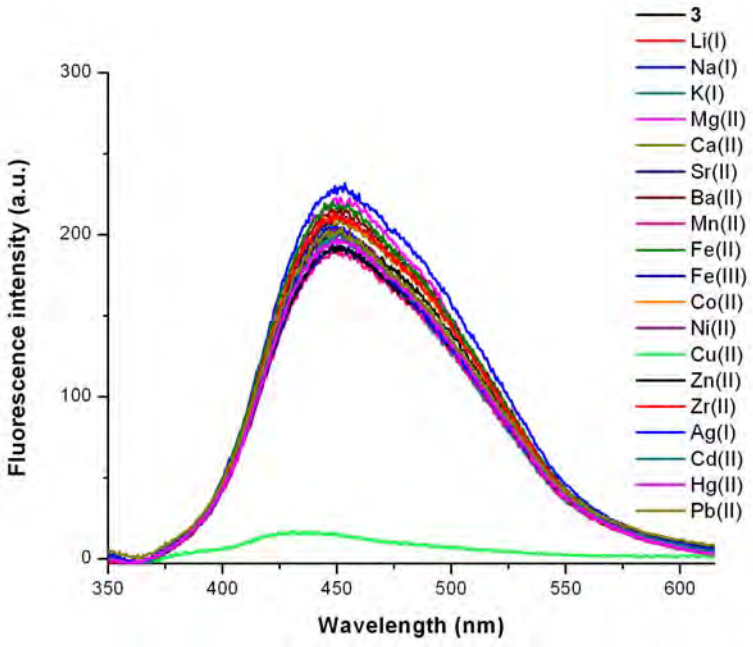

Figure 3.4 Fluorescence spectra of **3** (1 μM) in the presence of 19 metal ions (10 μM).

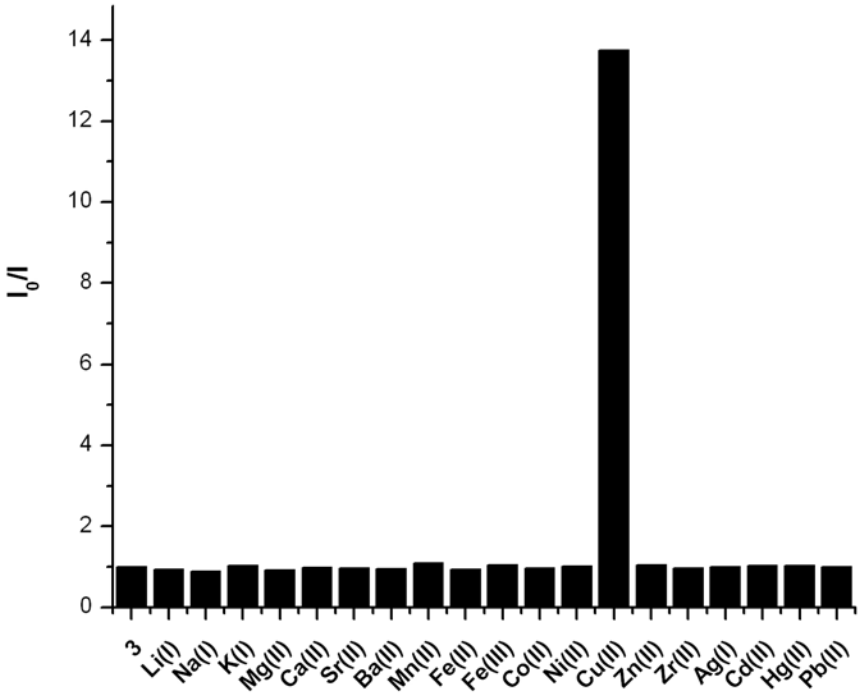

Figure 3.5 Fluorogenic responses of **3** with Cu(II) ions over metal ions (1 μM in 10 mM phosphate buffer pH 8.0) in the presence of 19 metal ions (10 μM)

3.4 Fluorescent titration of 3 with Cu^{2+}

In order to determine the sensitivity of flurophore **3**, the fluorescent titration with Cu^{2+} was conducted. Spectra in **Figure 3.6** and plot in **Figure 3.7** indicated that the fluorescent signal decreased dramatically when the ratio of **3** and Cu^{2+} are less than 1:3. With higher concentrations of Cu^{2+}, there is no significant change in signal quenching. This result suggested that the mechanism of fluorescent quenching should involve the chelation of the salicylate peripheries with Cu^{2+}. However, the first complexation of Cu^{2+} with the first salicylate group was affected the fluorescent signal more than the second and the third groups.

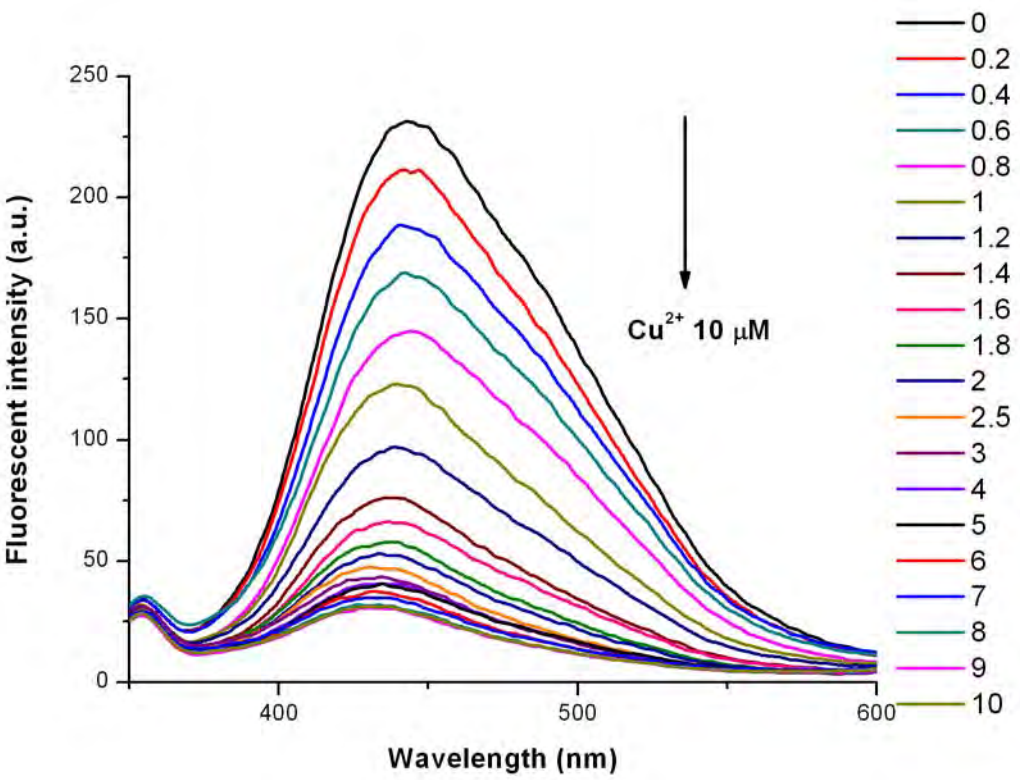

Figure 3.6 The fluorescence intensity of compound **3** (1 μM) with Cu(II) titration (0-10 eq.) in 10 mM phosphate buffer pH8.

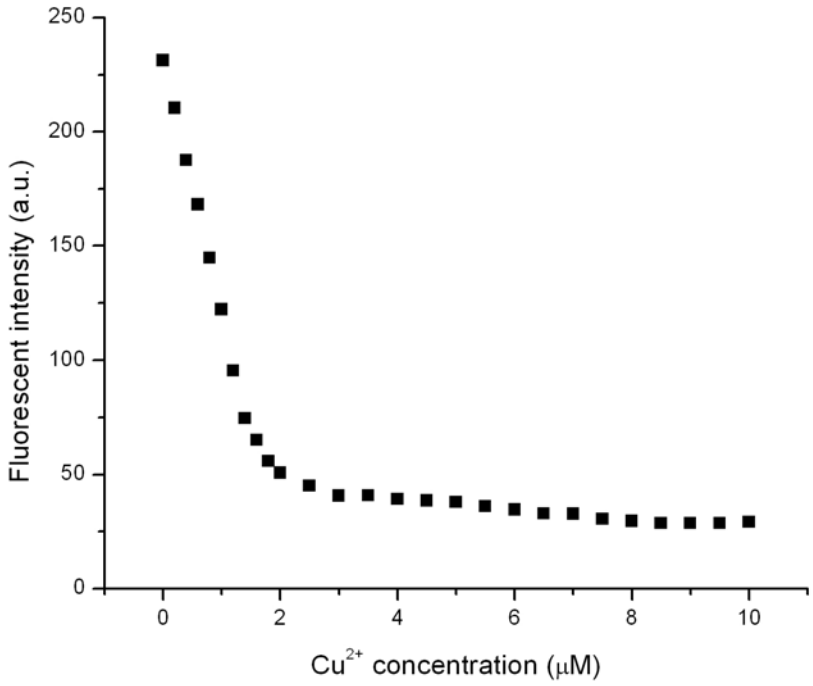

Figure 3.7 The fluorescence intensity of compound **3** (1μM) after added Cu^{2+} 0-10eq. in 10 mM phosphate buffer pH8.

3.5 The Stern-Volmer plot for fluorescent quenching of 3 by Cu^{2+}

By varying the concentration of Cu^{2+} and constructing a plot between (I_0/I) against the concentration of Cu^{2+}, a linear relationship with a slope of 1.62 x 10^6 M^{-1} was obtained. This slope corresponded to the Stern-Volmer constants (K_{sv}) (**Figure 3.8**) indicated that the efficient of **3** in quenching by Cu^{2+}.

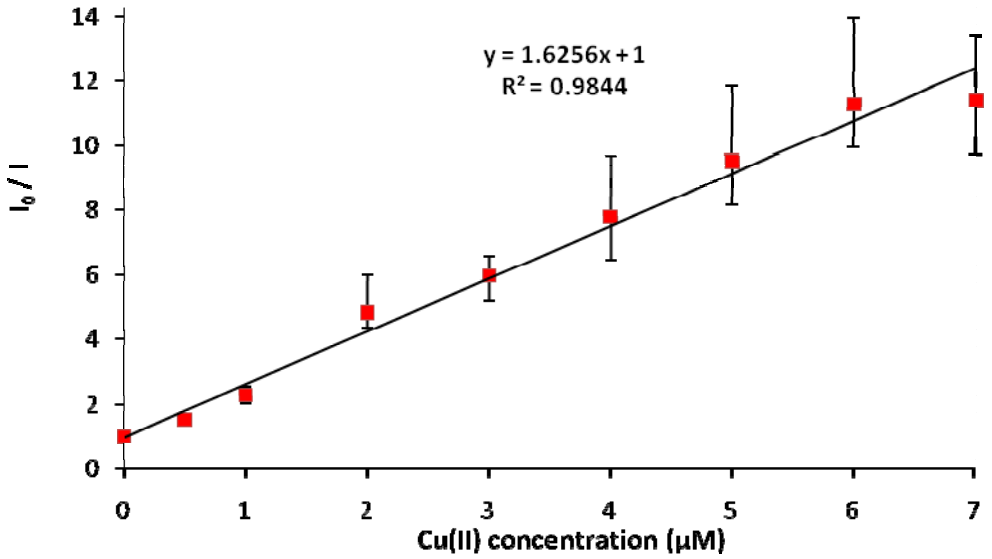

Figure 3.8 The Stern-volmer plot for fluorescent quenching of **3** by Cu^{2+} .

3.6 Effect of pH

The effects of pH on fluorescent intensity of fluorophore **1**-**3** were investigated using phosphate buffers of various pH (**Figure 3.9**). The signal of **1** was gradually increased at the pH values higher than **6** which are above the pKa of typical carboxylic acids (~4.0). For fluorophore **2**, a sharp increase in intensity was obtained when the pH is above 3.5. These data suggested that the ionization of one of the carboxylic acid groups in **1** could slightly facilitate its water solubility, while the ionization of one carboxylic acid group in **2** could strongly affect its solubility. For fluorophore **3**, the presence of hydroxyl groups enables the compound to be soluble under the pH lower than 3.5 by mean of protonation. For the experiment on **3** in the presence of Cu^{2+} (**Figure 3.10**), the fluorescent signals at pH below 3.5 were not

affected because of protonation of hydroxyl group. After deprotonation of carboxylate at pH 7-10, the fluorescent signal can appropriate for used as Cu^{2+} sensor.

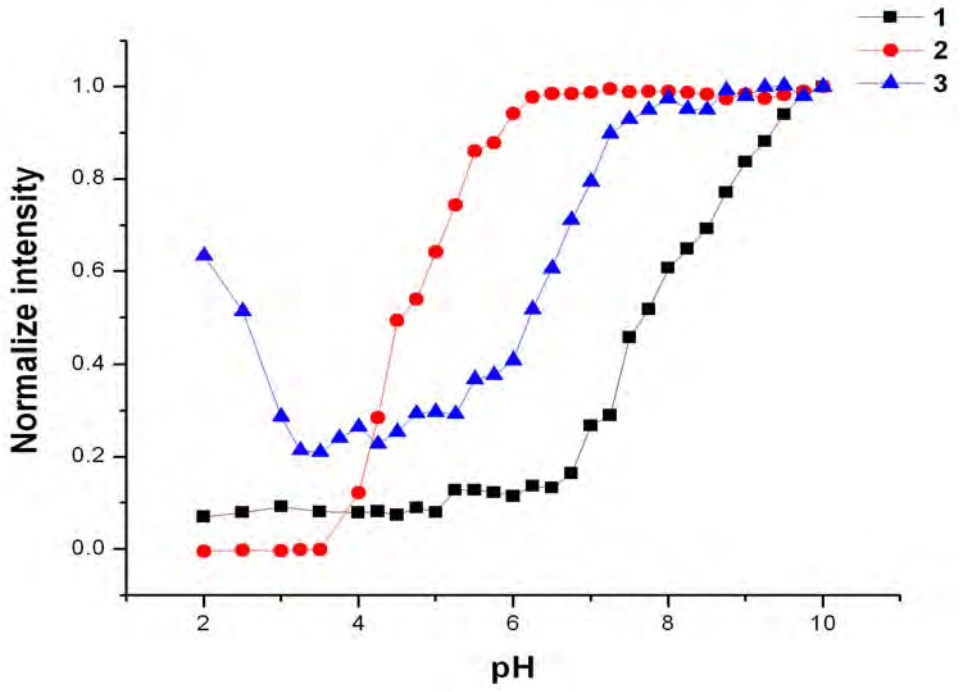

Figure 3.9 Effects of pH on fluorescent intensity of **1-3**

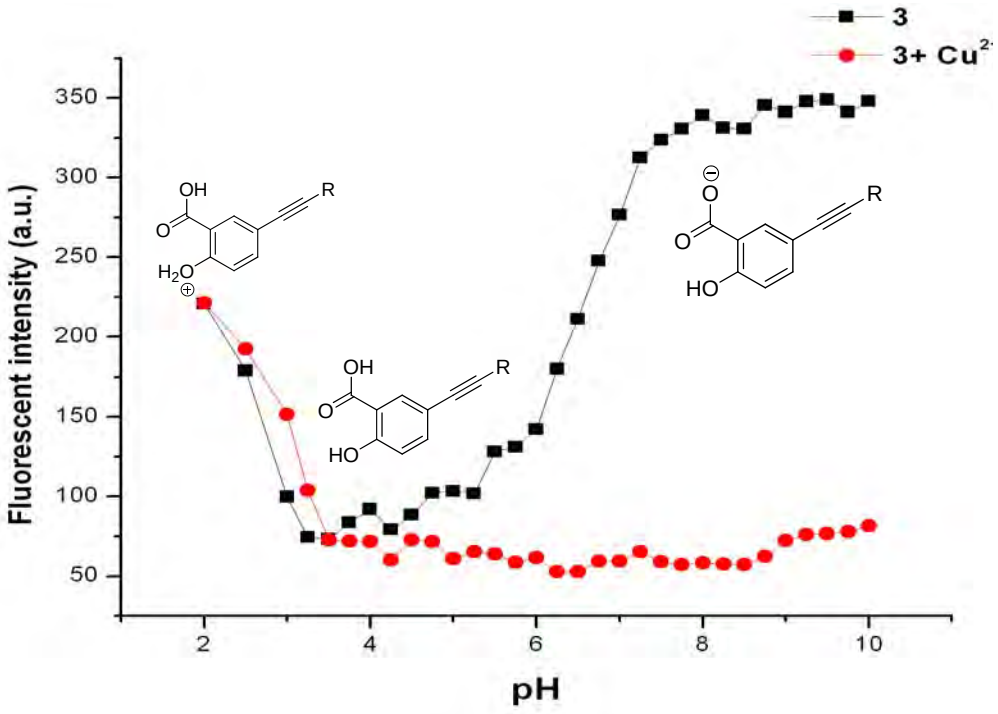

Figure 3.10 Effects of pH on fluorogenic response of **3** with Cu^{2+}

3.7 Competitive experiments

The selectivity for fluorophore **3** toward Cu^{2+} was further examined in a series of competitive experiments. The solution of **3** (1 μM) in phosphate buffer in the presence of Cu^{2+} (1 eq) was used as a blank. The quenching efficiencies in the presence of additional metal ions (10 eq) were not significantly different from the blank, which indicated that fluorophore **3** can be used as a selective sensor for Cu^{2+} without the interfering by a very high concentration of another metal ion in the same solution.

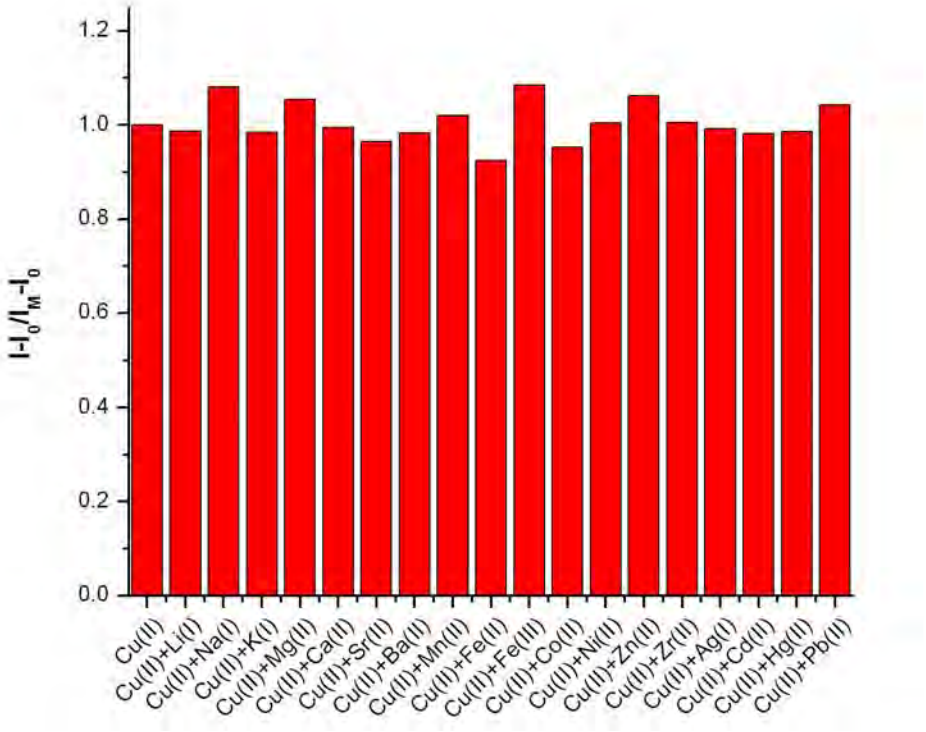

Figure 3.11 Competitive experiments of **3** (1 μM) and Cu^{2+} (1 μM) with 18 interfering metal ions (10 μM).

3.8 Fluorescence intensity amplification with surfactant

Even though fluorophore **3** exhibited a great selectivity toward Cu^{2+} in the presence of other metal ions, its weakly fluorescent nature may be of a disadvantage for the development of naked-eye sensors. According to a literature report, there have been some examples of fluorescent enhancement by using surfactants [12]. In this

study, the use of non-ionic surfactants appeared to be more feasible since the interaction between the surfactants and fluorophore **3** or metal ions should be minimized.

3.8.1 Surfactant selection

Three non-ionic surfactants including Brij 58 (CMC = 0.077 mM), Tween 22 (CMC = 0.08 mM), and Triton X-100 (CMC = 0.2 mM) were subjected to a screening test. The fluorescent signals of **3** in the presence of each surfactant (0.1 mM), both before and after the addition of Cu^{2+}, were shown in **Figure 3.12**. It is clearly demonstrated that the use Triton X-100 could provide an apparent differentiation for the systems with and without Cu^{2+}. Therefore, Triton X-100 was chosen for further studies. It is worth-noting that the concentration of Triton X-100 in this test was lower than the critical micelle concentration (CMC). The high concentration of Triton X-100 was found that had affected to lower sensitivity with Cu^{2+}. The appropriate amount of Triton X-100 will be discussed in section 3.8.2.

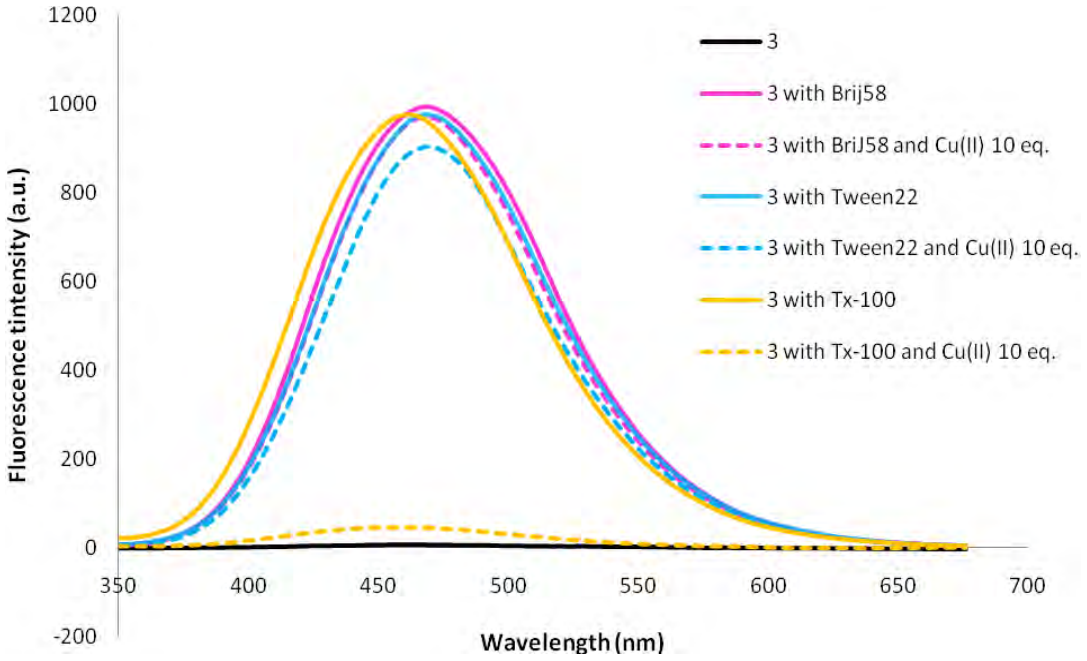

Figure 3.12 Effects of surfactants on fluorescent intensity of **3** and its reponses to Cu^{2+}.

3.8.2 Optimization of the surfactant concentration.

The amount of TritonX-100 used in the screening test (above) was below its CMC of 0.2 mM. In order to maximize the fluorogenic response toward Cu^{2+}, the concentration of surfactant had to be optimized (**Figure 3.13**). By comparing the fluorescence intensity of **3** in various concentrations of Triton X-100 (I_0), it was found that the concentration of 30 µM (0.03 mM) could provide the best quenching efficiency upon addition of Cu^{2+}. This result suggested that the fluorescent enhancement was not due to the micellar effect. The addition of non-ionic surfactant could only change the overall polarity of the medium, or interact with fluorophore **3** and limit its bond rotation upon excitation. At the concentrations more than 30 uM or above CMC (≥ 200 mM), the fluorescent signals were slighly quenched by Cu^{2+}, which indicated that the fluorescent enhancement by micellar effect might be a dominant process. The micelle formation may prohibit the accessibility of **3** toward Cu^{2+}.

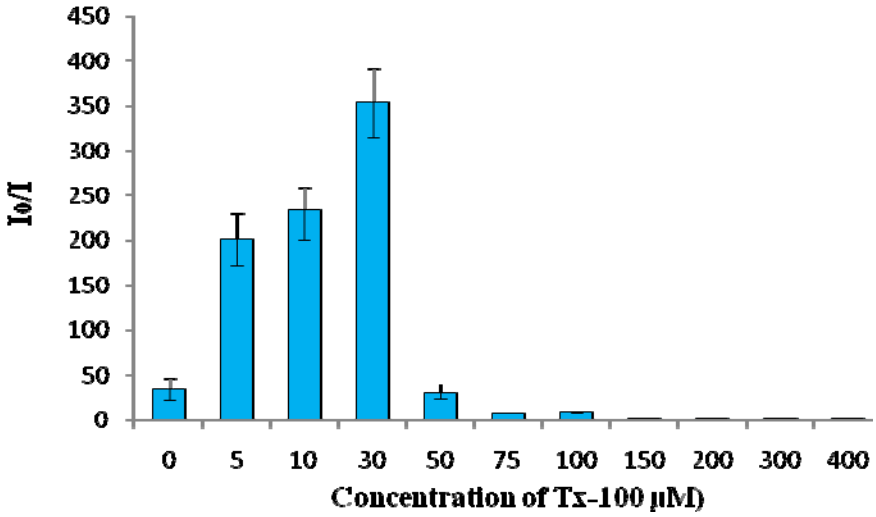

Figure3.13 Quenching efficiencies of **3** (1 µM) with Cu(II) (10 µM) under various concentrations of TritonX-100.

3.8.3 Stern-Volmer plot and detection limit in the presence of TritonX-100

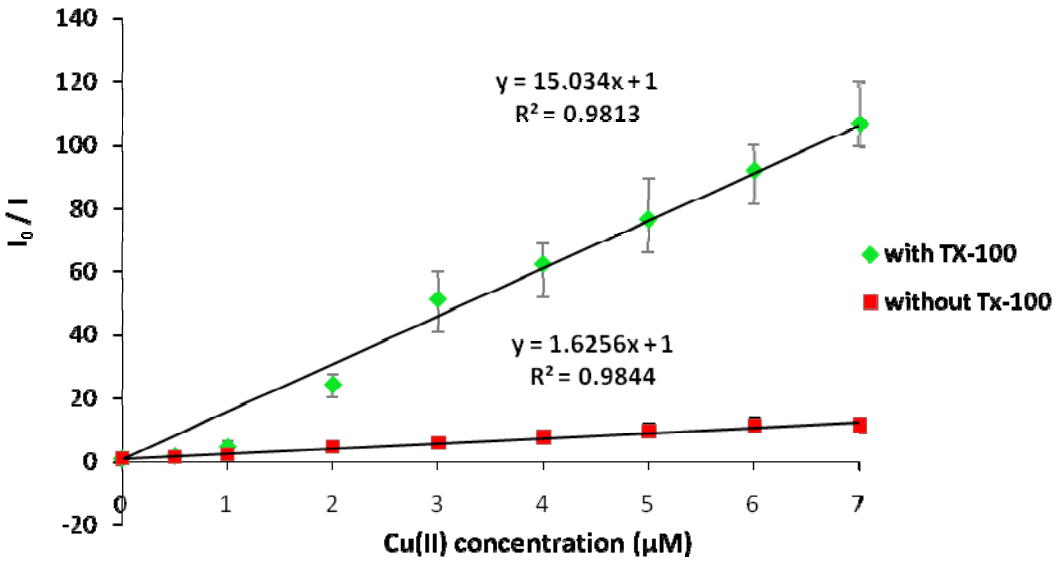

Figure 3.14 The Stern-Volmer plot of **3** with and without TritonX-100

A Stern-Volmer plot of the fluorescent quenching in the presence of Triton X-100 was then obtained by a series of experiments using various concentration of Cu^{2+}. The K_{SV} in the later case (1.50×10^7 M^{-1}) was approximately ten-fold of that from the system without surfactant (1.62×10^6 M^{-1}) (**Figure 3.14**). The high sensitivity led us to determine the detection limit of this analysis. Such value could be obtained by measuring the fluorescent intensity of **3** (1 µM) without Cu^{2+} ten times, then calculating the average and the standard deviation (SD) of those measurements (**Table 3.2**). The detection limit is concentration of Cu^{2+} at which the fluorescent intensity decreases three times of the standard deviation from the original average value, and could be calculated from the Stern-Volmer equation. In this case, the detection limit was calculated to be 3.10×10^{-9} M and 1.03×10^{-7} M for the system with and without Triton X-100, respectively.

Table 3.2 Sensitivity data for the system with and without surfactant.

System	Average I_0	SD	K_{SV} (M^{-1})	Detection limit	
				Molar	ppb
Without surfactant	46.44	2.21	$1.62x10^6$	1.03×10^{-7}	6.49
With surfactant	935.20	13.86	$1.50x10^7$	3.10×10^{-9}	0.19

3.8.4 EDTA

Finally, it would be interesting to see whether the quenched fluorescent signal could be completely restored by addition of a strong Cu^{2+} chelator. Ethylenediamine tetracarboxylic acid (EDTA) was chosen for this purpose as its complexation constant to Cu^{2+} is extremely high (log K_1 = 18.8). Data in **Figure 3.15** indicated that at least an equal molar ratio between EDTA and Cu^{2+} is required in order to obtain some signal restoration. The signal could be fully recovered when the amount of EDTA was approximately 30 μM, equivalent to three times of Cu^{2+} concentration. However, further addition of EDTA could slightly raise the signal higher than the original intensity. It was later confirmed that EDTA itself also enhance the fluorescent intensity of **3** to some extent.

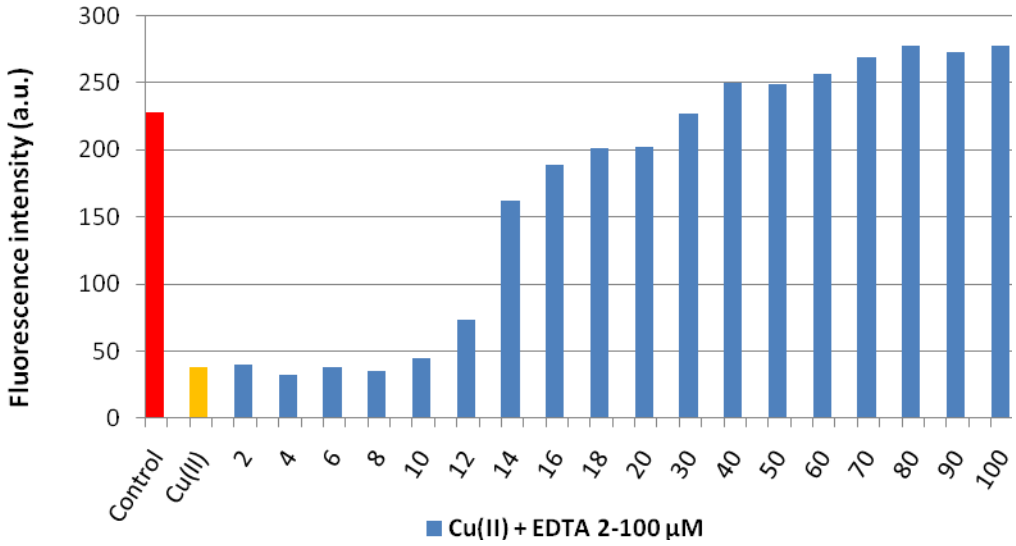

Figure 3.15 Effects of EDTA and the fluorescent restoration.

CHAPTER IV

CONCLUSION

4.1 Conclusion

Three water soluble fluorophores (**1**-**3**) were successfully synthesized. The synthesis relied on the Sonogashira coupling between the triiodotriphenylbenzene and the acetylenic aromatic ester. The comparison of photophysical properties of the compounds in phosphate buffer pH 8 indicated that the intramolecular charge-transfer (ICT) was responsible for the low quantum yield observed in the aqueous media, especially for fluorophore **3**. Addition of non-ionic surfactants, Triton-X 100, to the aqueous solution of **3** effectively increased the quantum efficiency, presumably by the reduction of the geometrical relaxation process. The fluorophore/TritonX-100 system could be developed into a highly sensitive Cu^{2+} sensor via a fluorescent quenching process. The selective quenching effect was probably associated with the electrostatic interaction between the Cu^{2+} and the salicylate groups appropriately positioned on the peripheries. The sensor also exhibited a great specificity to Cu^{2+} and the best detection limit achieved from the system with Triton X-100 was 0.19 ppb.

REFERENCES

[1] Lacowicz, J, Principles of Fluorescence Spectroscopy 3rd Ed. Springer Science, pp 1 – 25, New York, 2006.

[2] Liu, Y. Ogawa, K. Schanze, K. Conjugated polyelectrolytes as fluorescent sensors. Journal of Photochemistry and Photobiology C: Photochemistry Reviews. 10 (2009): 173–190

[3] Fana, J. Zhanga, Y. Murphya, B. C. Angell, E. S. Parkera, F. L. M. Flynna, R.B. et al. Fluorescent conjugated polymer molecular wire chemosensors for transition metal ion recognition and signaling. Coordination Chemistry Reviews.253 (2009) : 410–422

[4] Flaming K. Introduction to fluorescence theory and methods in Handout number 8: Techniques in biophysics 250.690, 2005.

[5] Kim, B. I. and Bunz, F. H. Modulating the Sensory Response of a Conjugated Polymer by Proteins: An Agglutination Assay for Mucury Ions in Water. Journal of the American Chemical Society. 128 (2006): 2818-2819.

[6] He, L. C. Ren, L. F. Zhang, B. X. Dong, Y. Y. and Zhao, Y. A Fluorescent Chemosensor for Copper (II) Based on a Carboxylic Acid-functionalized Tris(2,2'-bipyridine)-ruthenium (II) Complex. Analytical Sciences. 22 (2006): 1547-1551

[7] Weng Q. Y. Teng L. Y. Yue, F. Zhong, R. Y. and Ye H. B. A New Selective Fluorescent Chemosensor for Cu(II) ion Based on Zinc Porphyrin-Dipyridylamino. Inorganic Chemistry Communications. 10 (2007): 443-446

[8] Ha-Thi, M. H. Penhoat, M. Michelet, V. and Leray, I. Highly Selective and Sensitive Phosphane Sulfide Derivative for the Detection of Hg^{2+} in an Organoaqueous Medium. Organic Letters. 9 (2007): 1133-1136.

[9] Tolosa, J. Zucchero, J. A. Bunz, F. H. Water-Soluble Cruciforms: Response to Protons and Selected Metal Ions. Journal of the American Chemical Society. 130 (2008): 6498-6506.

[10] Jung, S. H. Kwon, S. P. Lee, W. J. Kim, J. Hong, C. S. Kim, W. J. and et al. Coumarin-Derived Cu^{2+}- Selective Fluorescence Sensor: Synthesis,

Mechanisms, and Application in Living Cells. Journal of the American Chemical Society. 131 (2009): 2008-2012.

[11] Xu, Z. Beak, H. K. Kim, N. H. Cui, J. Qian, X. Spring, R. D. and et al. Zn^{2+}-Triggered Amide Tautomerization Produces a Highly Zn^{2+}- Selective, Cell- Permeable, and Ratiometric Florescent Sensor. Journal of the American Chemical Society. 132 (2010): 601-610.

[12] Niamnont, N. Siripornnoppakhun, W. Rashatasakhon, P. and Sukwattanasinitt, M. A Polyanionic Dendritic Fluorophore for Selective Detection of Hg^{2+} in Triton X-100 Aqueous Media. Organic Letters. 11 (2009): 2768-2771.

[13] Plater, J. M. McKay, M. and Jackson, T Synthesis of 1,3,5-tris[4 (diarylamino)phenyl]benzene and 1,3,5-tris(diarylamino)benzene derivatives. Journal of the Chemical Society Perkin Transactions 1. (2000): 2695-2701.

[14] Simpson, D. C. Mattersteig, G. Martin, K. Gherghel, L. Bauer, E. R. Rader, H. J. and et al. Nanosized Molecular Propellers by Cyclodehydrogenation of Polyphenylene Dendrimers. Journal of the American Chemical Society. 126(2004): 3139-3147.

[15] Duggan, M. E. Duong, L. T. Fisher, J. E. Hamill, T. G. Hoffman, W. F. Huff, J. R. et al. Nonpeptide. Nonpeptide αvβ3 Antagonists. 1. Transformation of a Potent, Integrin-Selective αIIbβ3 Antagonist into a Potent αvβ3 Antagonist. Journal of Medicinal Chemistry. 43 (2000) 3736-3745.

[16] Aujard, I. Baltaze, J. P. Baudin, J. B. Cogne, E. Ferrage, F. Jullien, L. and et al. Tetrahedral Onsager Crosses for Solubility Improvement and Crystallization Bypass. Journal of the American Chemical Society. 123 (2001) 8177-8188.

[17] Agback, K. H. Ahrgren, L. Berglindh, T. Haraldsson, M. Olsson, L. I. and Smedegaard, G. Novel substituted salicyclic acids. WO 9310094 A1 19930527.

[18] Esfandiari, N. H. Navidpour, L. Shadnia, H. Amini, M. Samadi, N. Faramarzi, M. A. et al. Synthesis, antibacterial activity, and quantitative structure-activity relationships of new (*Z*)-2-(nitroimidazolylmethylene)-3(2*H*)-benzofuranone derivatives. Bioorganic and Medicinal Chemistry Letters. 17 (2007) 6354-6363.

APPENDIX

APPENDIX

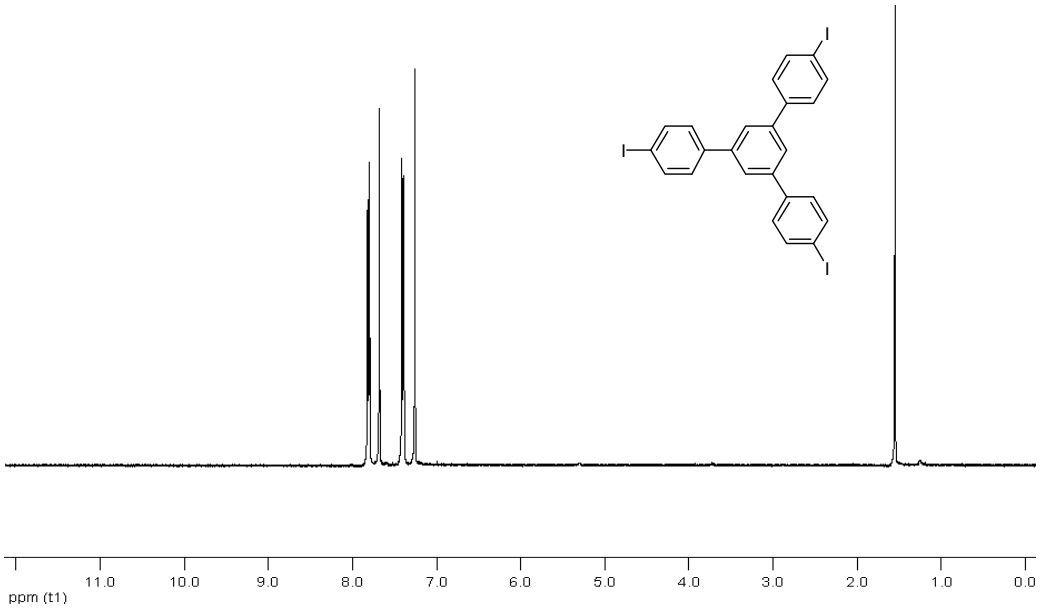

Figure 1 ^{1}H-NMR spectrum of *1,3,5-Tris-(4-iodophenyl)-benzene* (**4**)

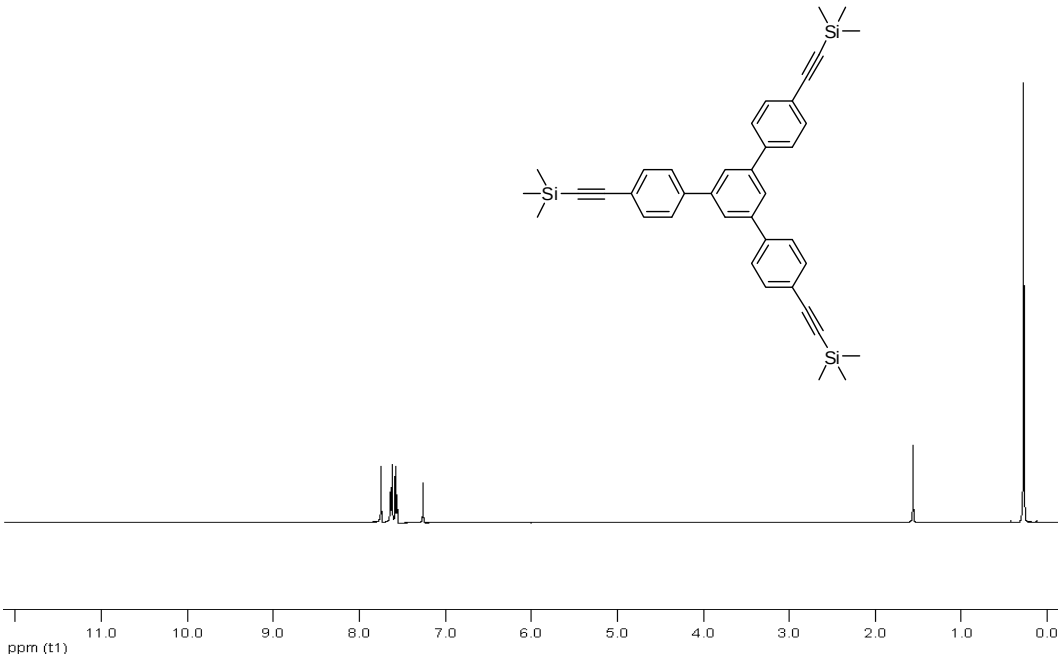

Figure 2 ^{1}H-NMR spectrum of *Tris-(4-trimethylsilylethynyl-phenyl)-benzene* (**5**)

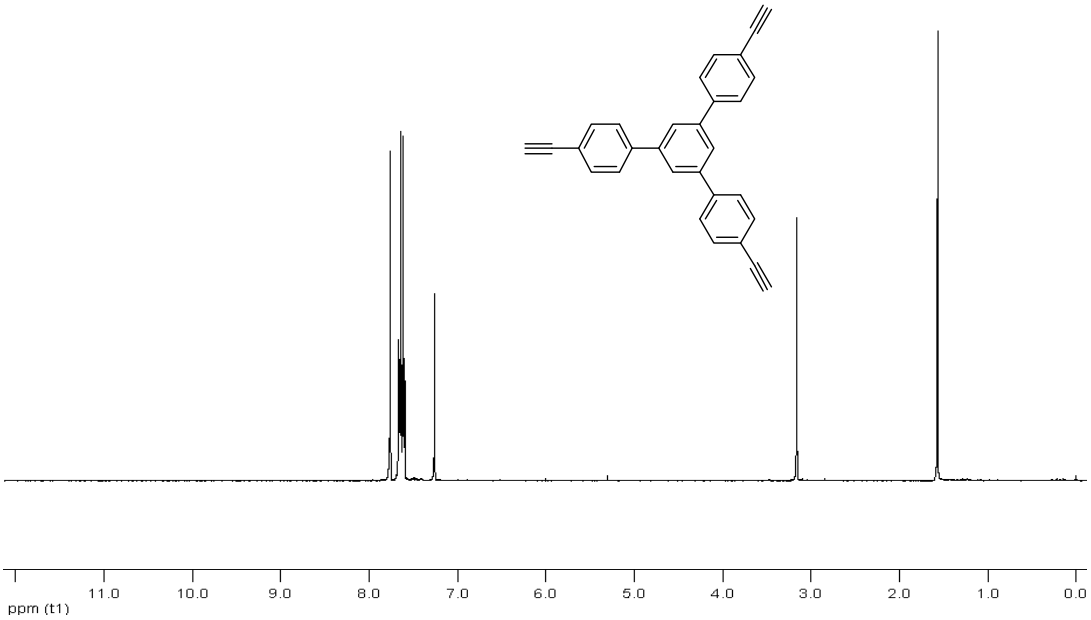

Figure 3 ^{1}H-NMR spectrum of *1,3,5-Tris-(4-ethynyl-phenyl)-benzene)* (**6**)

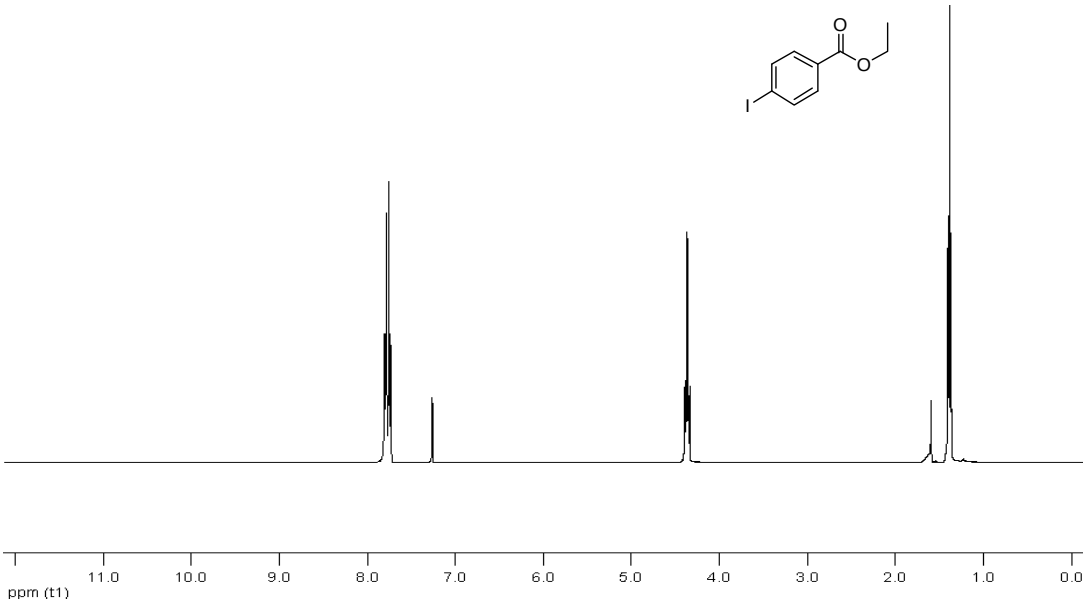

Figure 4 ^{1}H-NMR spectrum of ethyl 4-iodobenzoate

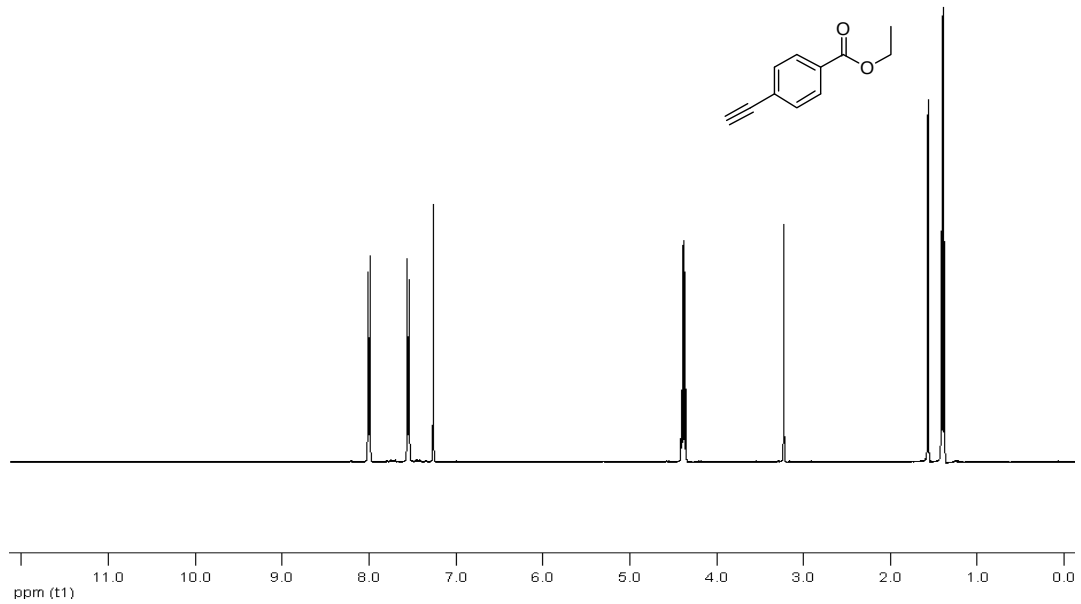

Figure 5 ^{1}H-NMR spectrum of ethyl 4-ethynylbenzoate

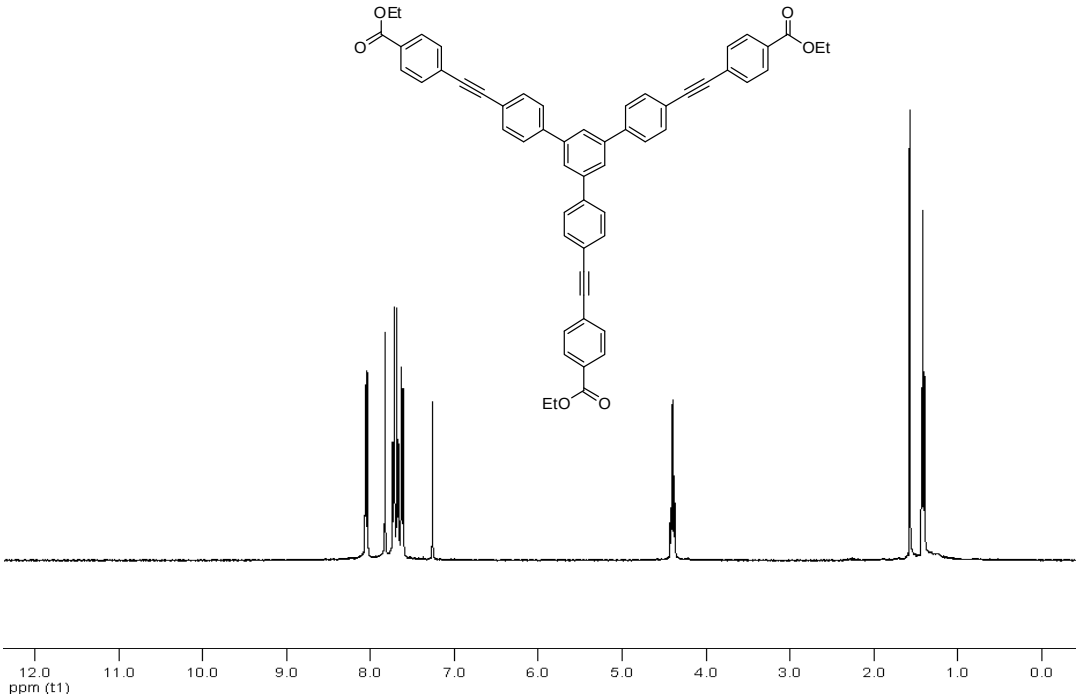

Figure 6 ^{1}H-NMR spectrum of *Triester* (7)

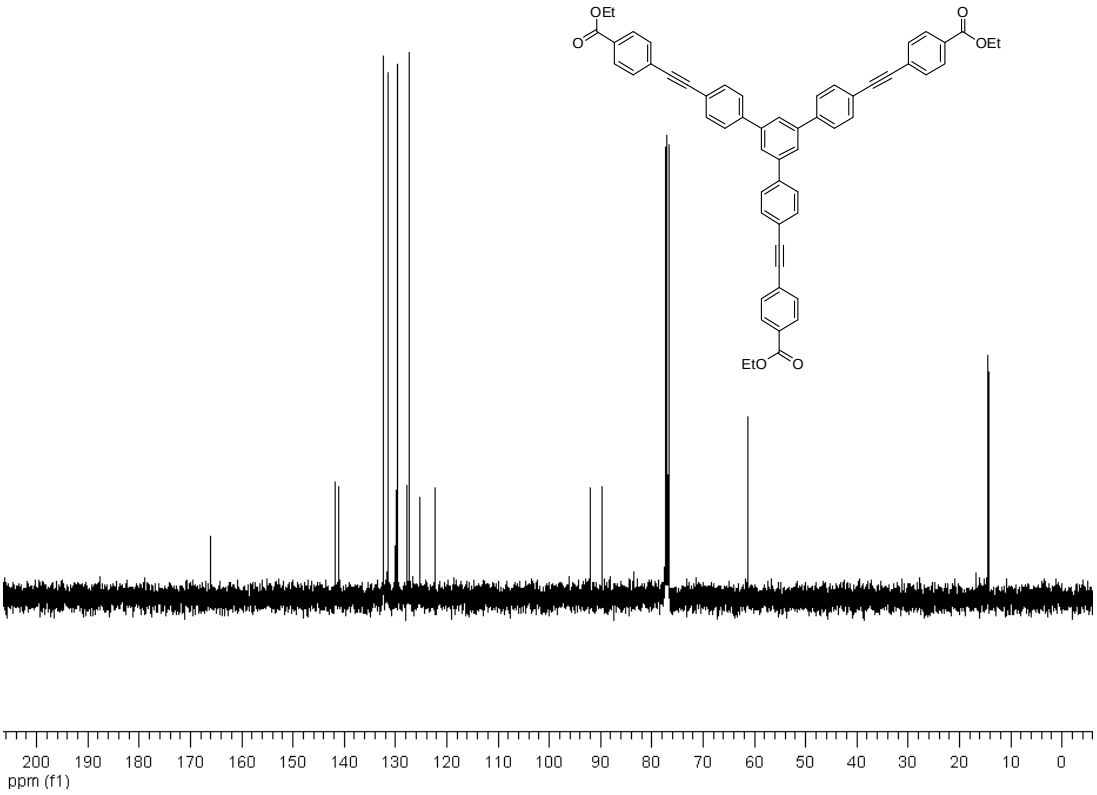

Figure 7 ^{13}C-NMR spectrum of *Triester* (7)

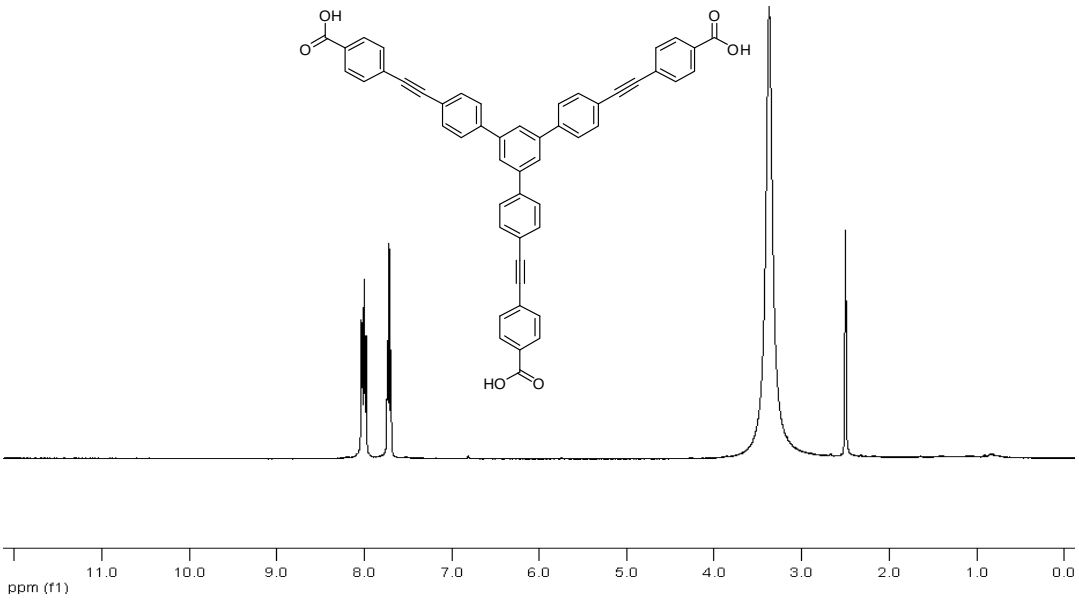

Figure 8 ^{1}H-NMR spectrum of *compound 1*

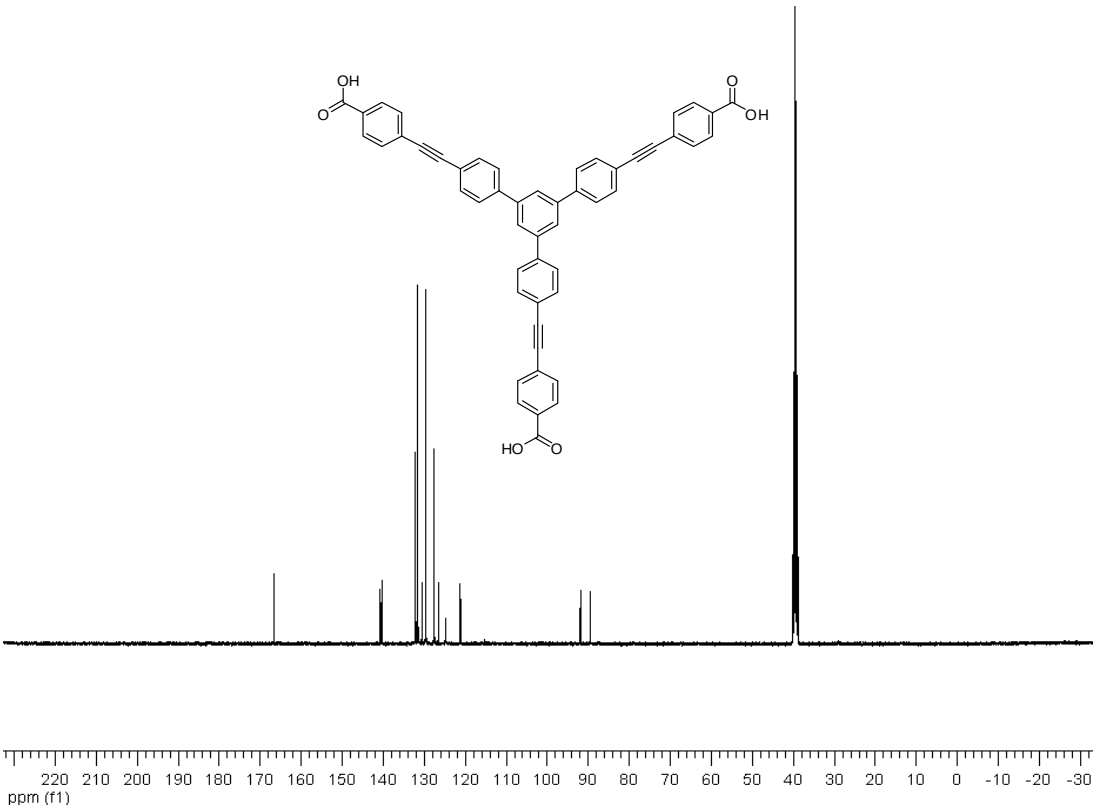

Figure 9 ^{13}C-NMR spectrum of *compound 1*

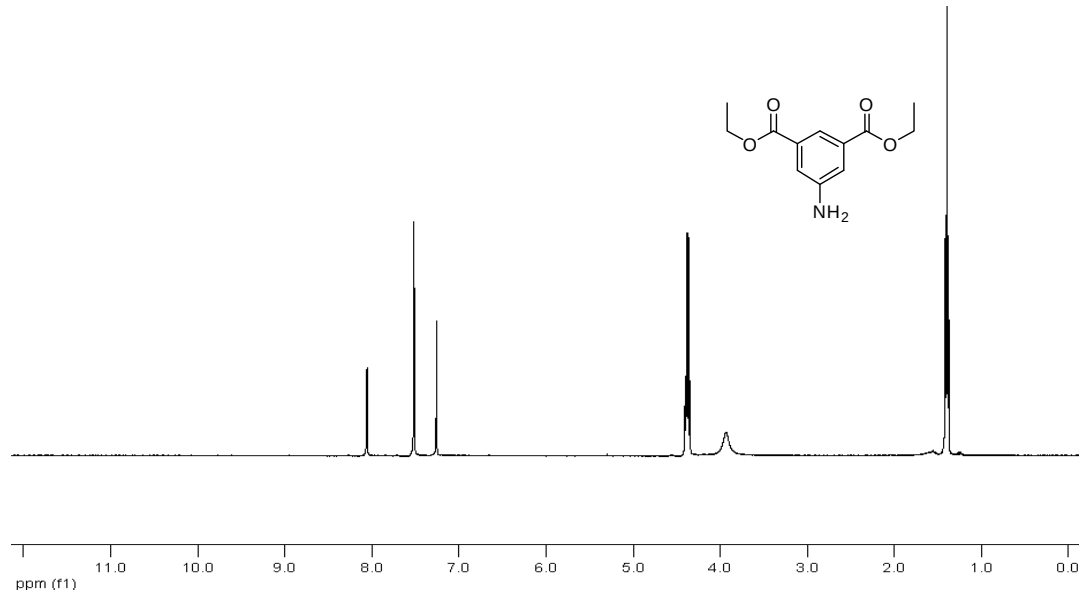

Figure 10 ^{1}H-NMR spectrum of diethyl 5-aminoisophthalate

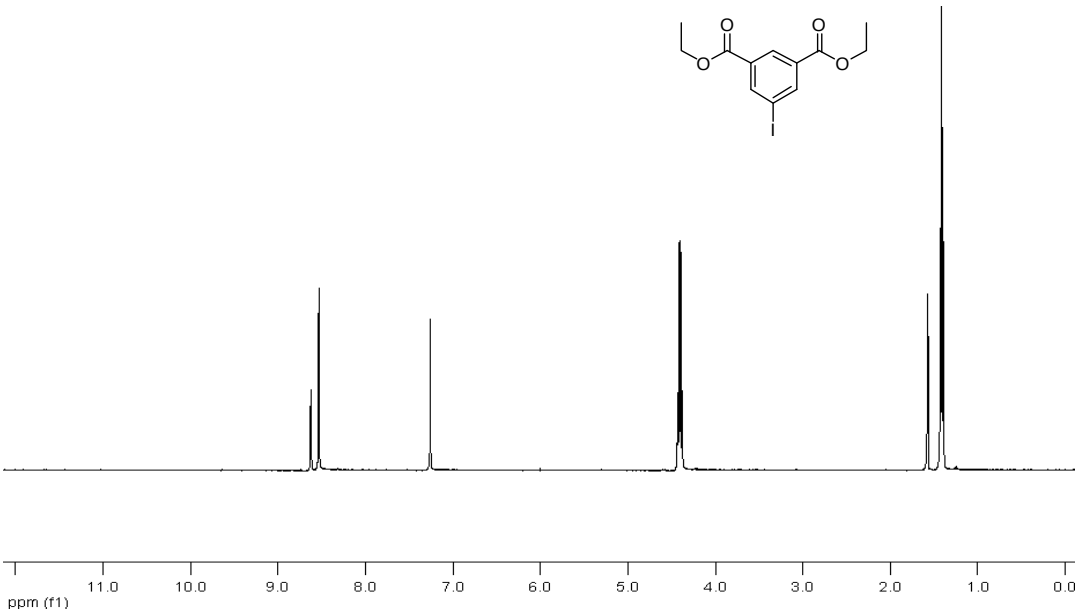

Figure 11 ^{1}H-NMR spectrum of diethyl 5-iodoisophthalate

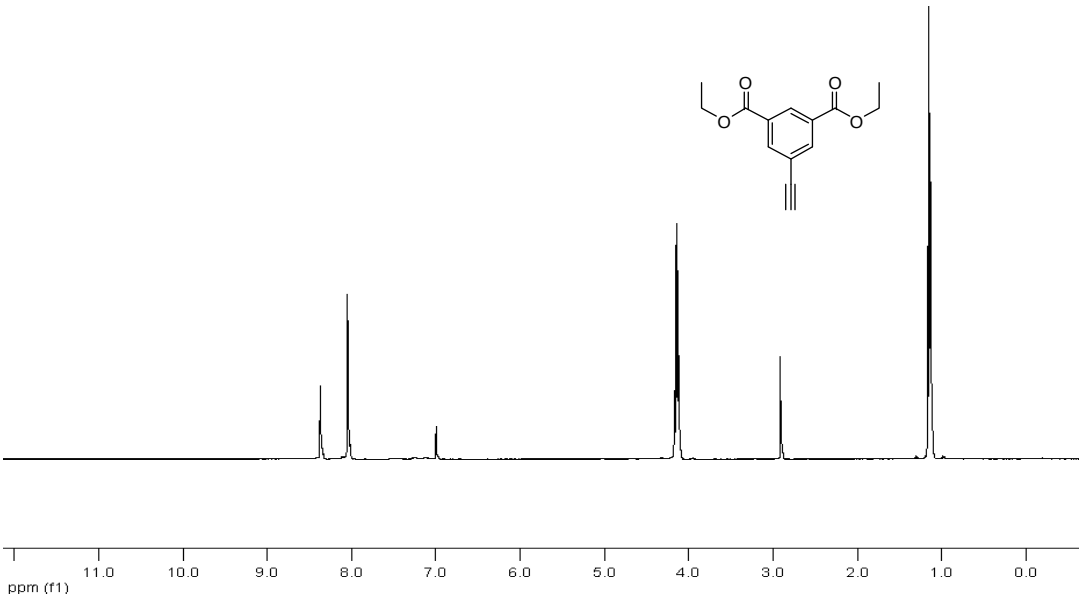

Figure 12 ^{1}H-NMR spectrum of diethyl 5-ethynylisophthalate

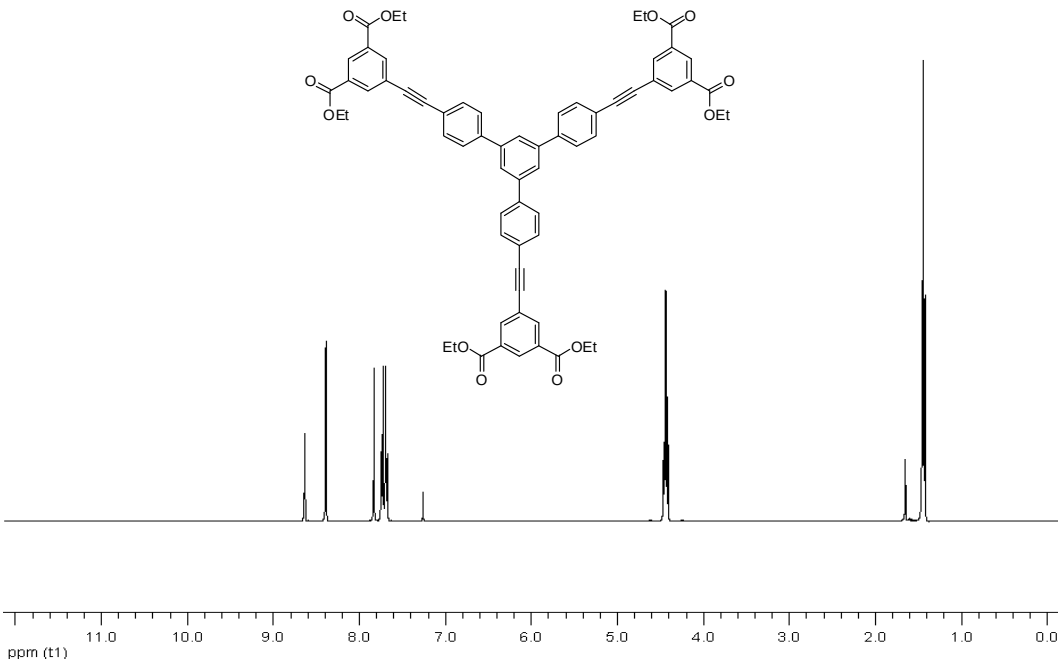

Figure 13 ^{1}H-NMR spectrum of *Hexaester* (8)

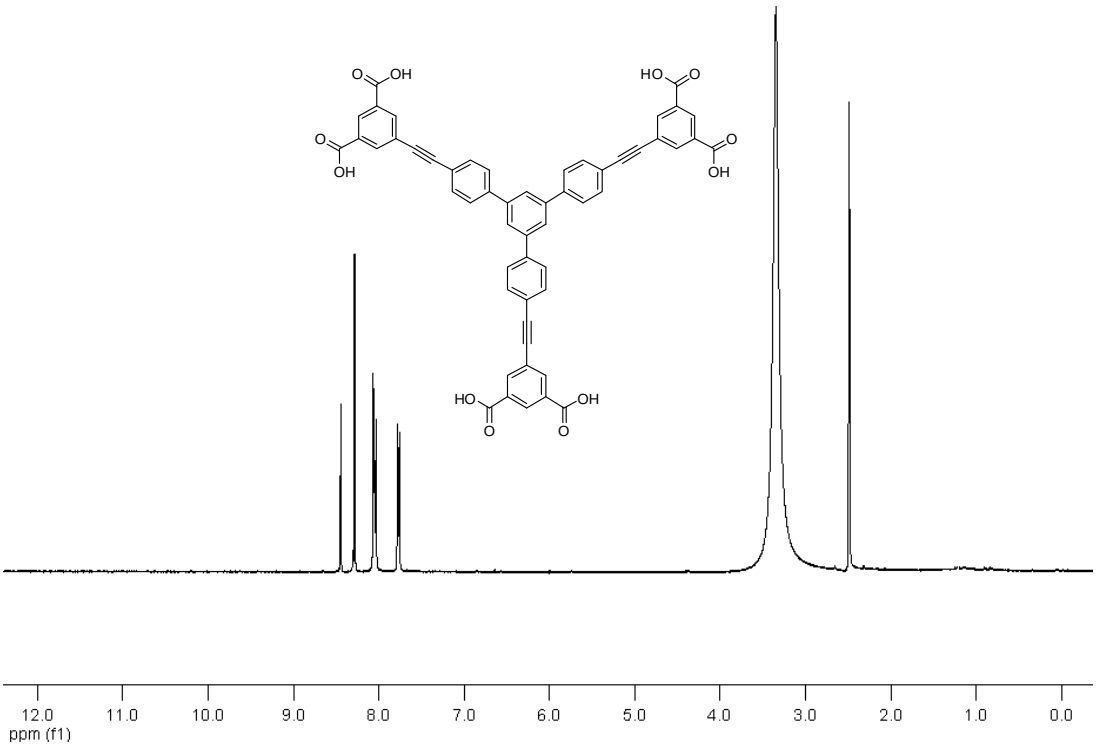

Figure 14 ^{1}H-NMR spectrum of *Compound 2*

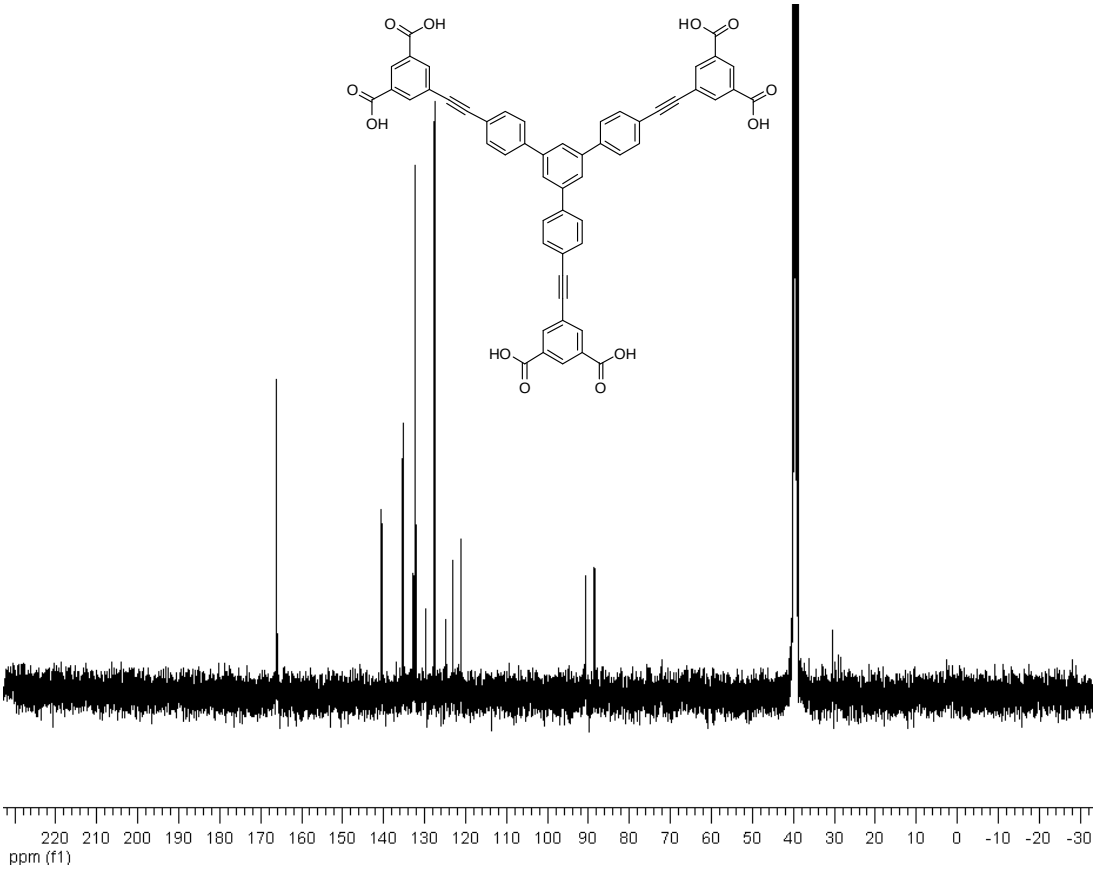

Figure 15 ^{13}C-NMR spectrum of *Compound 2*

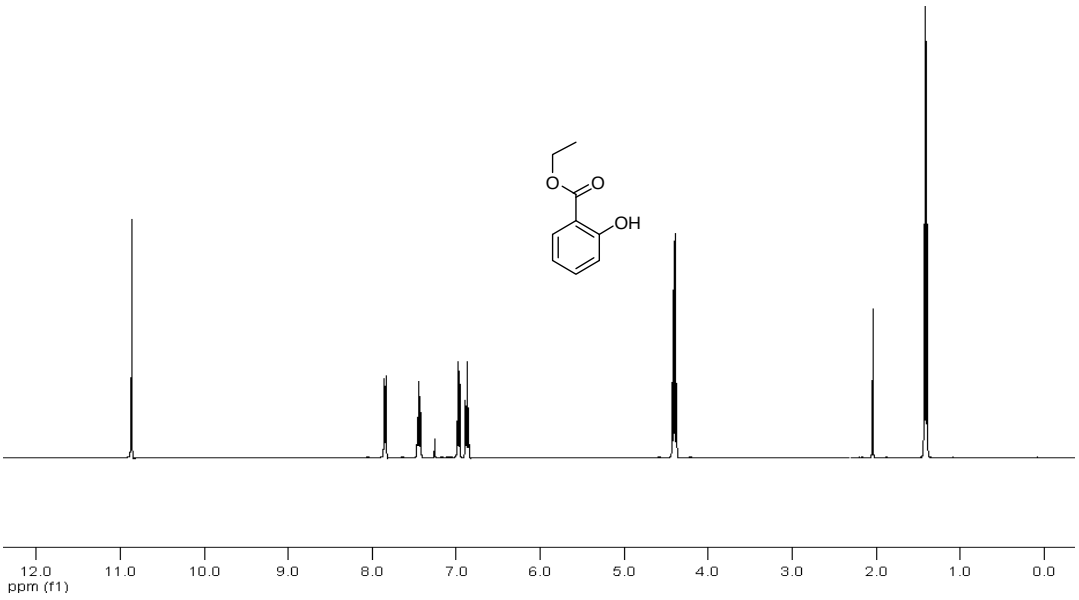

Figure 16 ^{1}H-NMR spectrum of *ethyl 2-hydroxybenzoate*

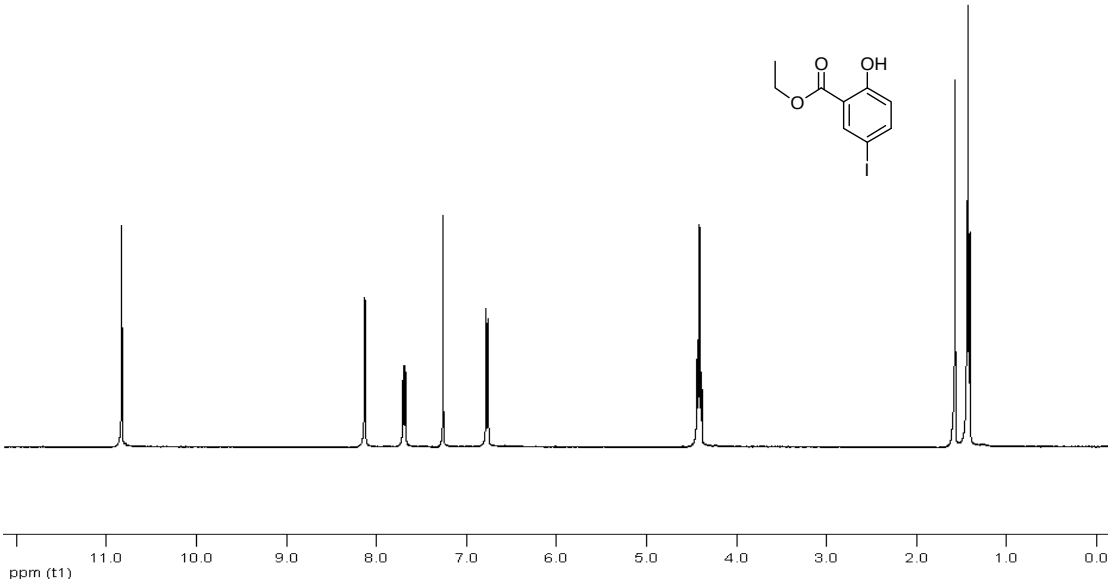

Figure 17 ^{1}H-NMR spectrum of *ethyl 4-iodobenzoate*

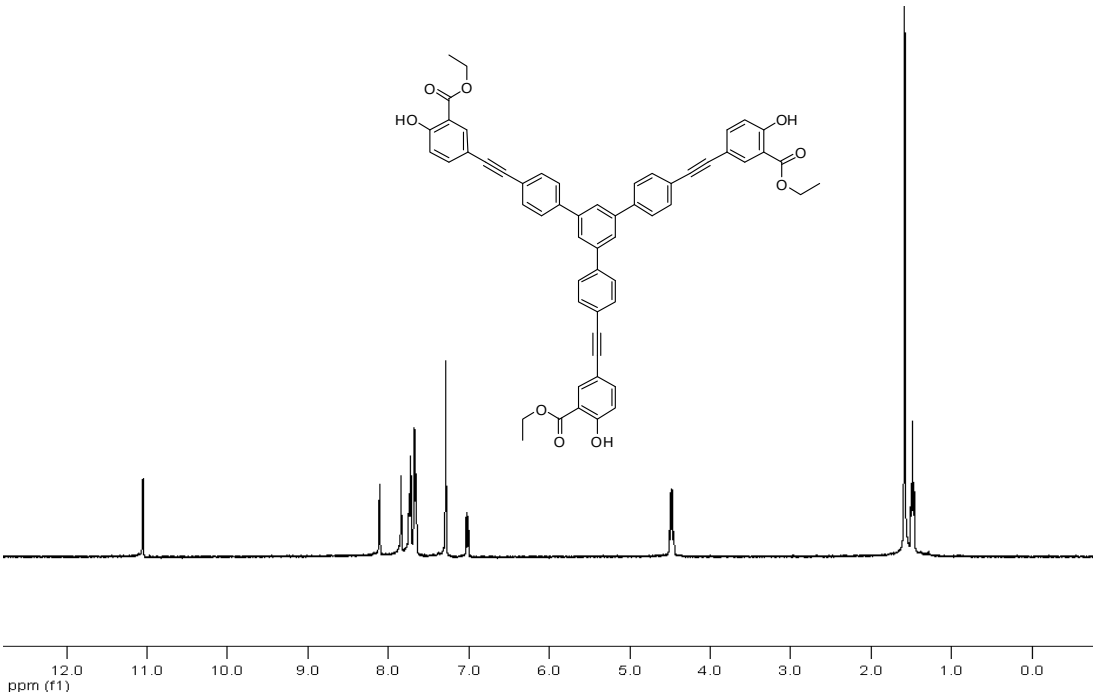

Figure 18 ^{1}H-NMR spectrum of *Tri-salicylate ester* (9)

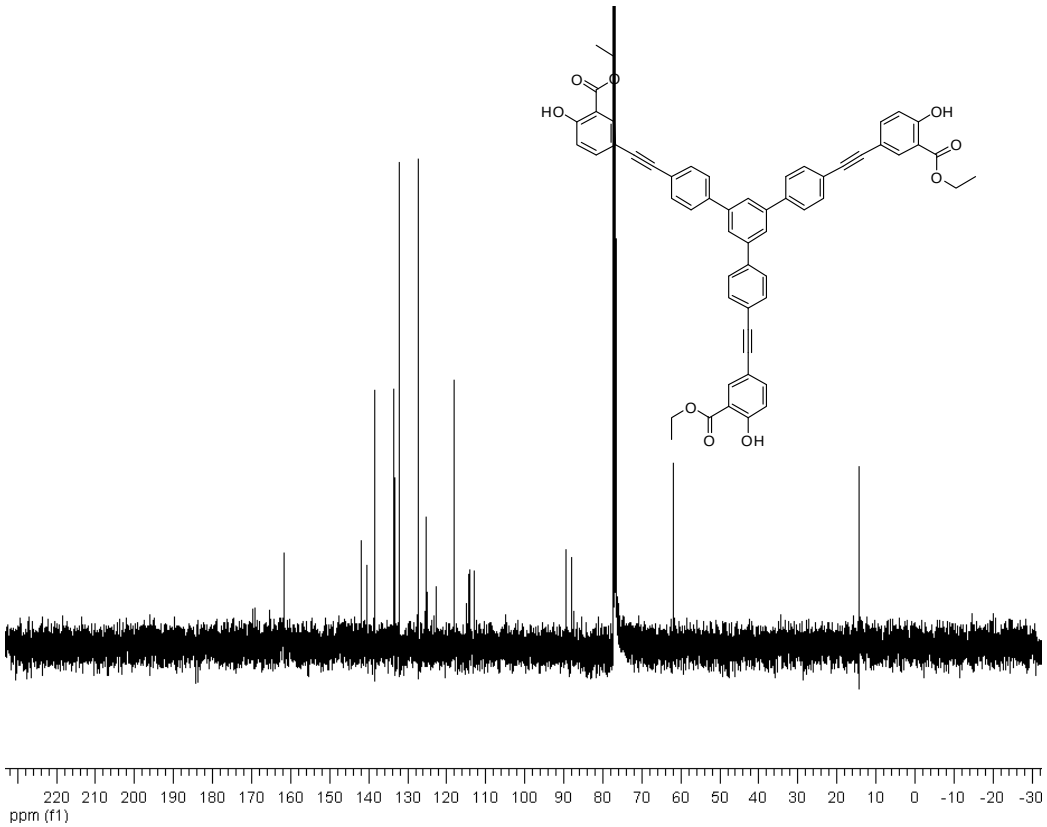

Figure 19 ^{13}C-NMR spectrum of *Tri-salicylate ester* (9)

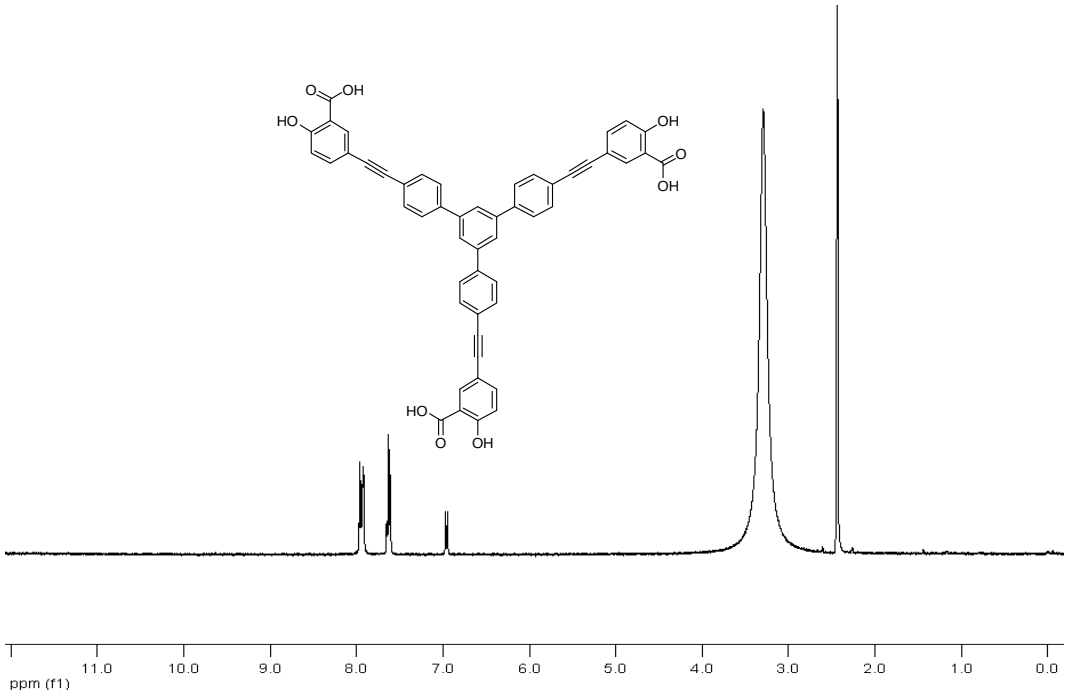

Figure 20 ^{1}H-NMR spectrum of *compound 3*

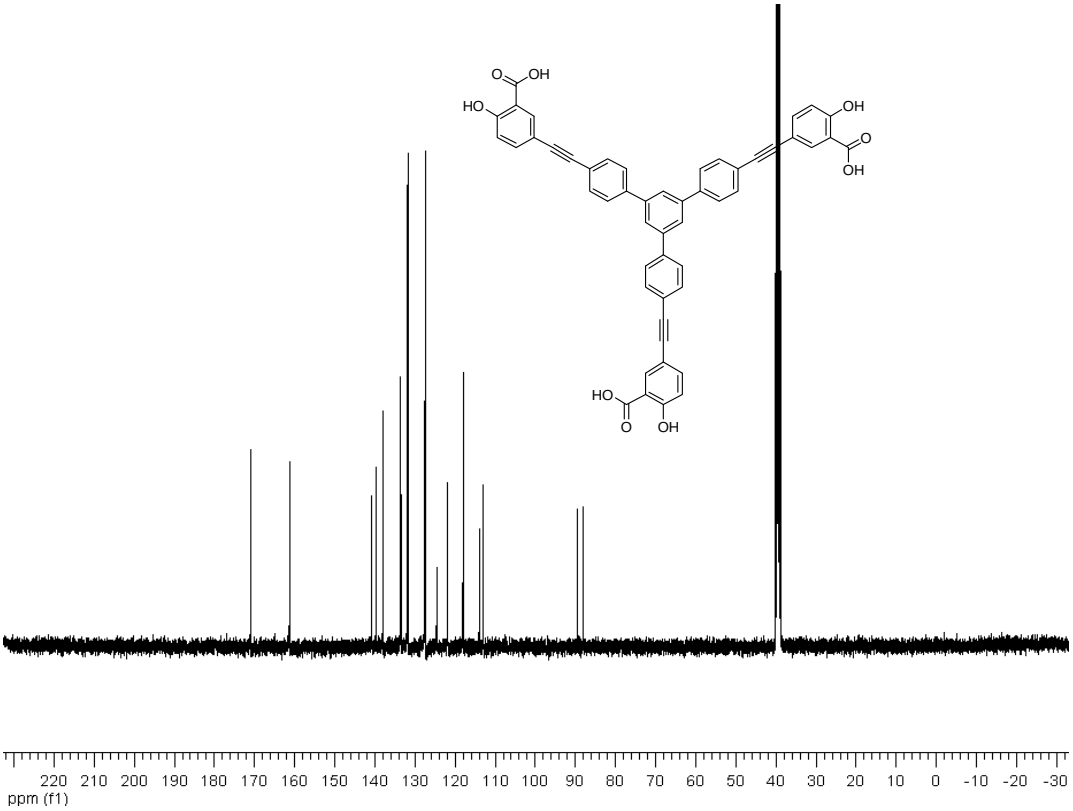

Figure 21 ^{13}C-NMR spectrum of *compound 3*

VITAE

Mr. Sakan Sirilaksanapong was born on October 22, 1984 in Nakhonsithammarat, Thailand. He got a Bachelor's Degree of Science in Chemistry from Mahidol University in 2006. In 2007, he started his a Master's Degree in Petrochemistry and Polymer Science program a Chulalongkorn University. During he had presented "Synthesis of Water-Soluble Fluorescent Dendrimers From Triphenylbenzene Derivatives" in Pure and Applied Chemistry International Conference (PACCON 2010) and "Triphenylbenzene-ethynylene Dendritic Fluorophores" in Pure and Applied Chemistry International Conference (PACCON 2011), by poster presentation.

His address is 177/82 Moo 4, Ratchapruk 1 Village, Paknakhon Road, Muang, Nakhonsithammarat, 80000 Thailand, tel. 086 9797048.